NPL REPORT CMAM 61

REPORT

Development, validation and publication of a complete theoretical model for hydrophone/amplifier transfer characteristics

Pierre Gélat, Roy Preston and Andrew Hurrell

February 2001

NPL
National Physical Laboratory

NPL Report CMAM 61

February 2001

Development, validation and publication of a complete model for hydrophone/amplifier transfer characteristics

Pierre Gélat, Roy Preston and Andrew Hurrell*

Centre for Mechanical and Acoustical Metrology
National Physical Laboratory
Teddington
Middlesex
United Kingdom
TW11 0LW

*Precision Acoustics Ltd, Spur E Government Buildings,
Prince of Wales Road, Dorchester, Dorset DT1 1PY

ABSTRACT

A complete theoretical model for the transfer characteristics of a 25 µm film thickness 0.5 mm diameter bilaminar hydrophone has been developed and validated as part of project 4.4.3 of the DTI National Measurement System Programme for Acoustical Metrology, 1998-2001.

The model includes:

- the possibility to model one-dimensional acoustic propagation in multi-layered media using a transfer matrix formulation
- secondary piezoelectric effects
- the electrical effects of the leg, modelled as a distributed series resistance/shunt lossy capacitance network
- the hydrophone coaxial cable, modelled as a transmission line, followed by a load if required
- the amplifier transfer characteristics, the properties of which are to be obtained from measurement.

Precision Acoustics Ltd has contributed to this project by producing measurements of some of the model input parameters.

The open-circuit response predicted by the model compares well with calibration results and varying the model input parameters within plausible ranges appears to reproduce the trends observed in the responses of calibrated devices.

ISSN 1369-6785

National Physical Laboratory
Teddington, Middlesex, UK, TW11 0LW

Approved on behalf of the Managing Director, NPL,
by Graham Torr, Head, Centre for Mechanical and Acoustical Metrology

CONTENTS

0. PROJECT DETAILS

0.1 PURPOSE

This report carried out by the National Physical Laboratory (NPL) in partnership with Precision Acoustics (PA) Ltd for the DTI National Measurement System Policy Unit describes a project to **Develop, validate and publish a complete theoretical model for hydrophone/amplifier transfer characteristics**. It is project 4.4.3 of the DTI National Measurement System Programme for Acoustical Metrology,1998-2001.

The objective of the project is:-

- to support UK industry and the NHS by assisting them in improving the accuracy of hydrophone measurements, particularly in the field of medical ultrasound.

The team has conducted the project in two phases:-

- Phase 1. A literature review and investigation of different available theoretical approaches, followed by a survey of key end users and technical authorities to establish their precise requirements;
- Phase 2. Development of a full theoretical model and its validation.

0.2 CHANGES IN PROJECT TEAM

PA replaced Marconi Technology Centre as NPL's project partner before the project got underway. It was planned that Marconi would establish reference physical data for membrane hydrophones for use in the theoretical model to be developed in the project. The expertise and resources of PA being more limited than those of Marconi, it was necessary to re-consider the allocation of tasks. It was decided that PA would:

- Undertake the initial survey of requirements by contacting interested parties (originally to be done by NPL).
- Contribute with NPL to the establishment of basic physical properties of pvdf (originally to be done by Marconi).
- Establish membrane hydrophone constructional reference (originally to be done by Marconi).
- Contribute to the establishment of reference devices (originally to be done by Marconi).

1 INTRODUCTION

1.1 BACKGROUND AND DRIVERS

Ultrasonic imaging is still the most rapidly growing medical imaging modality, and the complexity of the acoustical fields generated by the equipment continually poses new measurement challenges. One of the main methods of measurement and characterisation of medical ultrasonic fields propagating in water is through the use of calibrated hydrophones. Some of the main drivers for hydrophone measurements and calibrations are:-

- enabling UK manufacturers to comply with the regulatory requirements of the USA Food and Drug Administration (FDA) 510(k) Reporting Requirements (1) - an essential requirement for access to the USA market;
- enabling manufacturers and end users, such as medical physics departments, to undertake measurements to current and future international specification standards such as IEC 61157 (2), IEC 61102 (3) and IEC 61266 (4);
- enabling manufacturers to comply with future specification standards which will underpin the regulatory requirements of the EC Medical Devices Directive (5);
- enabling manufacturers to maintain quality control during production of equipment;
- enabling research workers to establish reference exposure data for biological effects studies;
- enabling UK instrument manufacturers to provide high quality calibrated hydrophones to customers world-wide.

Over the last 15 years, the demands placed on hydrophone-based measurement systems have gradually increased. This can be appreciated by examining the measurements required for compliance with specification standards and the use of the resulting measured values. In general, the manufacturer of medical ultrasonic equipment will need to compare measured values of ultrasonic quantities, or derived quantities, with pre-set limits for a variety of reasons, including:-

- to ensure overall levels set down by USA FDA 510(k) are not exceeded;
- to ensure the levels established in IEC 61157 for pre-declaration exemption are not exceeded;
- to ensure correct attribution of the safety class of ultrasonic fields in future international ultrasonic field safety standards;
- to ensure products are within quality control limits.

As these requirements have grown over the last few years, so too have the demands placed on measurement systems.

1.2 ACCURACY OF REQUIREMENTS

The acoustical quantities which have to be measured or derived are either acoustic pressure, intensity or power. When acoustic intensity or power are derived from acoustic pressure, the uncertainties are double those of the primary quantity acoustic pressure because intensity is proportional to the square of the acoustic pressure in a plane wave. Typically, the specification standards require manufacturers to achieve uncertainties in intensity measurements of ±20-25% or better. Uncertainties in the primary measurand, acoustic pressure, must therefore be less than half these figures, disregarding other sources of uncertainty, which themselves can be significant. This means that the uncertainty in the calibration of a hydrophone should ideally be less than ±10%. Currently, the typical uncertainty in the calibration of a hydrophone at NPL, traceable to national standards, is ±5% at 2-5 MHz, increasing to ±11% at 20 MHz. At these frequencies, and for narrow-band measurements, these uncertainties may be acceptable. However, even at the lower frequencies where the bulk of the industrial measurements are made, there are a number of sources of error associated with measurements of diagnostic imaging and Doppler ultrasonic fields which are attributable to the system frequency response. These errors, which can amount to many percent or tens of percent, increasingly need to be addressed. There are also other errors associated with hydrophones not being omni-directional, and these too need to be considered.

1.3 ‘GOLD STANDARD’ MEMBRANE HYDROPHONES

Ever since the early developments of hydrophones for measurement purposes, it has been realised that the first priority in addressing errors is to use high quality measuring devices: devices with a smooth and flat frequency response, small active element compared with the ultrasonic wavelength, which are stable and reproducible. Hydrophones which have been developed to meet the requirements of medical ultrasound are either of the needle or membrane type, both using polyvinylidene fluoride as the piezoelectric sensing element. Overall, the relatively poor performance of needle hydrophones has led to a number of specification standards, and most notably the US FDA Reporting Requirements (1), limiting the type of hydrophone that can be used in absolute field characterisation to membranes. Although there are now a number of suppliers of such hydrophones world-wide, membrane hydrophones produced by Marconi Technology Centre, and jointly developed with NPL, are recognised as the ‘gold standard’ measuring devices. Figure 1.1 shows a typical bilaminar membrane hydrophone.

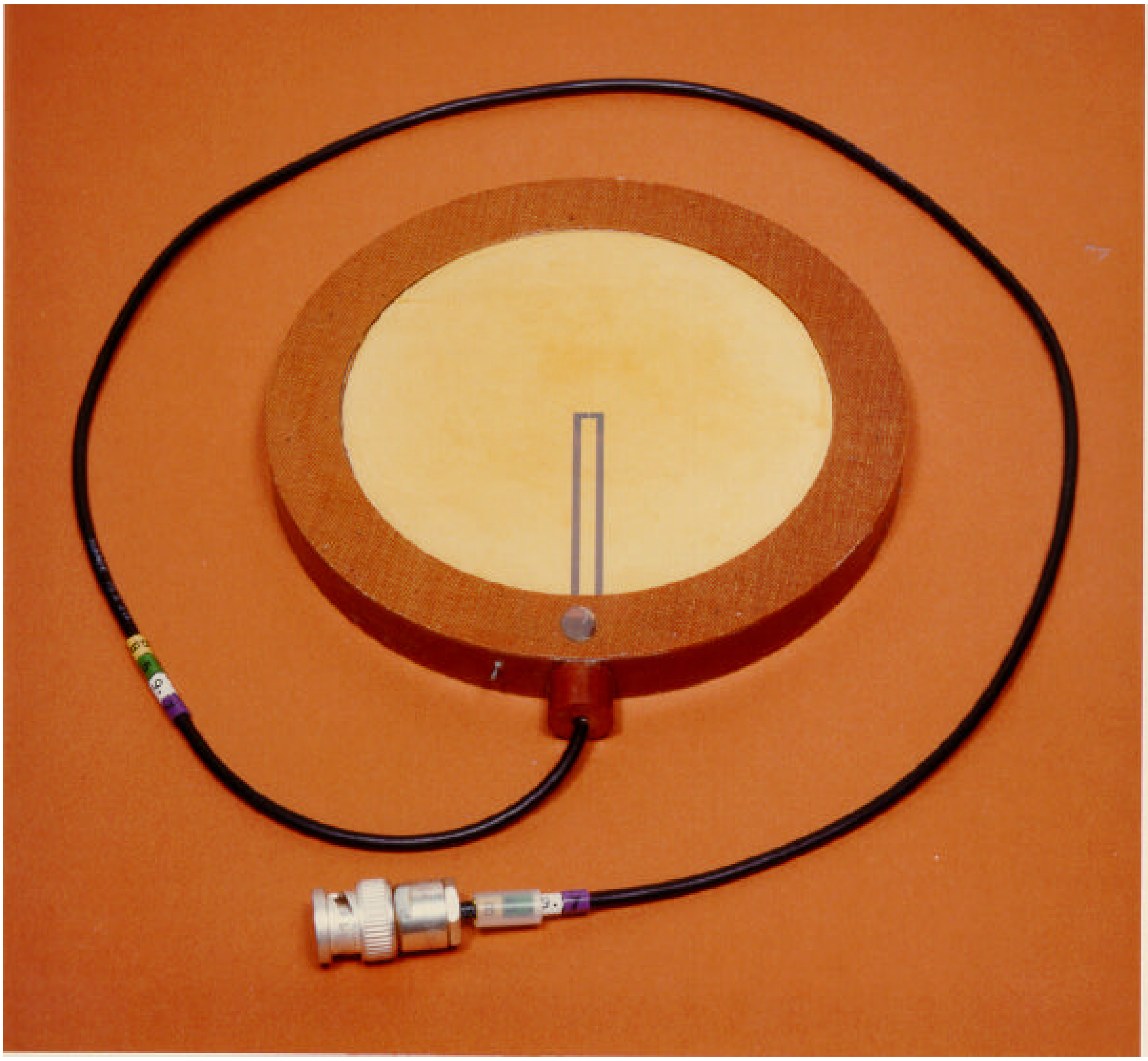

Figure 1.1: A bilaminar membrane hydrophone.

1.4 THE NEED FOR HYDROPHONE MODELS

The long-term stability and smooth frequency response of membrane hydrophones are two of the key features which have contributed to their acceptance as the 'gold standards'. Another reason is that the device is conceptually simple and some of its important performance characteristics can be predicted. A basic theoretical model for a membrane hydrophone was established many years ago (6) and this model has been very valuable in supporting the development of measurement standards for a number of reasons:-

- it has allowed extrapolation of calibration data beyond the frequency range of the primary standard, albeit with significantly increased uncertainties;

- during the development of hydrophones with smaller active elements, the model was used to study methods of offsetting the decrease in sensitivity of membrane hydrophone by adjustment of the design of the electrode shielding (7);
- during recent developments to extend the frequency range of NPL's primary standard laser interferometer (the source of traceability for hydrophone calibrations) to 60 MHz , the theoretical modelling was a useful guide to progress (8).

Originally, the model was developed and tested for coplanar-shielded membrane hydrophones, devices consisting of a single sheet of pvdf. Increasingly, however, the bilaminar-shielded hydrophone, consisting of two laminated sheets of pvdf, has become the hydrophone of choice and the industrial standard. Although the model has been applied to bilaminar devices, the main limitation is that it is not sufficiently 'complete'. Certain physical characteristics of the bilaminar construction are represented generically in the model. As these characteristics relate to the electrode structure which is sandwiched between the two sheets of pvdf, they cannot be measured for a particular hydrophone without destroying it. Furthermore these characteristics differ between the different types of bilaminar device. There is therefore a need to gain an improved knowledge of these characteristics in order to improve the accuracy and the versatility of the model, resulting in a need for a more 'complete' model for membrane hydrophones.

1.5 REQUIREMENTS FOR HYDROPHONE MODELS

Originally, the users of NMS hydrophone calibration services required only the sensitivity of the hydrophone at the acoustic working frequency of the ultrasonic field being measured. For narrow-band measurements this need could be met by using a single numerical value for the sensitivity of the hydrophone at the appropriate ultrasonic frequency. However, for any realistic measurements made of the ultrasonic fields generated by an imaging or pulsed Doppler system, the measured waveform would contain a broad spectrum of signals over a large frequency range, mainly caused by nonlinear propagation effects in the water path. Unfortunately, the bilaminar hydrophone, which is employed for this type of measurement because it can be used in ordinary tap water and exhibits good signal-to-noise ratio, has a sensitivity which gradually increases with frequency. This increase in response affects the measured waveform (9). For a typical 3.5 MHz nonlinearly distorted waveform, this increased response would lead to an error of 15-19% (10) in the value for the temporal-average intensity, one of the critical quantities required for compliance with regulatory standards. It has therefore become crucially important to address this source of error.

The true acoustic pressure waveform can in principle be derived from the measured waveform through a process of deconvolution providing the impulse response of the hydrophone is known. This impulse response can be determined from knowledge of the magnitude and phase response of the hydrophone over the range of relevant frequencies, information that has not been available to the user of hydrophones. Furthermore, the process of deconvolution is not a procedure which can easily be implemented at the industrial user level. This was realised some years ago within the IEC and so, to provide a method of correcting for limited bandwidth hydrophones, a simple fitting process was specified (11). This involves a graphical fitting procedure to correct a measured waveform, a process which has been found to be inaccurate.

Deconvolution is the preferred route, as this will lead to improved accuracy of the correction procedure. For this, the magnitude and phase response of the hydrophone is needed. Currently, the standard NPL calibration certificate provides values for the sensitivity of the hydrophone over a range of frequencies but no phase information. This information can only be used if it is assumed that the relative phase varies linearly with frequency and that the user has the ability to deconvolve the hydrophone response from the measured signal. Improvements are in hand as one of the projects proposed for the next NMS Acoustics Programme 2001-2004 is to first develop and then provide a relative phase calibration service for hydrophones. However, even though initial magnitude and phase response data will become available, accuracy over the required frequency range may limit the usefulness of the deconvolution process as considerable validation may be required.

The existence of a full theoretical model of a particular type of membrane hydrophone would allow the user to take experimental waveforms and deconvolve the hydrophone response in order to determine the true acoustic pressure waveform, a process which would allow quantitative assessment of measurement errors and uncertainties. It would further allow the inverse process, a procedure known as convolution. By convolution of a theoretical waveform with the impulse response function given by the hydrophone model, it would be possible to compare theoretical results with experiment, again providing a greater insight into measurement errors and uncertainties.

1.6 MODELLING FOR MATCHED HYDROPHONE/AMPLIFIERS

An intermediate approach to deconvolution is to compensate for the increase in the sensitivity of the hydrophone with frequency by the use of a signal amplifier whose gain changes with frequency by an equal and opposite amount. The development of the ‘matched amplifier’ approach has been very successful, to the point that the majority of hydrophones supplied by Marconi Technology Centre were matched to such devices. The matching of the amplifier to a particular hydrophone takes place during the standard calibration of the membrane hydrophone at NPL. The method used to set the gain of the matched amplifier is simple and not optimised for any particular measurement situation. A reliable mathematical model of the hydrophone and amplifier responses would allow the matching process to be optimised. The benefit of this optimisation process would be to allow the hydrophone/amplifier combination to be used to achieve greater accuracy in the measurement of nonlinearly distorted and broadband ultrasonic fields. Even though the hydrophone/amplifier will represent an improved measurement system, there is still a need to determine residual measurement uncertainties and corrections, again a task possible if a reliable model for the transfer function of the combination is known.

1.7 SUMMARY

Over the last two years there has been a significant growth in the number of hydrophones required by customers to be calibrated in conjunction with NPL-designed matched amplifiers. This is driven by the need of customers to improve the accuracy with which they determine intensity, currently typically no better than ±25% (95% confidence). A more complete theoretical model for a membrane hydrophone and matched amplifier would enable:-

- application of deconvolution techniques to a measured waveform in order to establish the true acoustic pressure waveform;
- application of convolution techniques to a theoretically determined, or a reference experimentally measured, waveform in order to establish estimates of the uncertainties in the measurement of acoustical quantities;
- comparison of theoretical and experimental waveforms;
- determination of optimum characteristics of amplifiers for hydrophone/amplifier combinations;
- quantitative optimisation of the matching process for amplifiers.

The benefits of a more complete theoretical model for a membrane hydrophone and matched amplifier would be:-

- reduced industrial costs resulting from improved uncertainties in ultrasonic field measurements;
- increased accuracy and quality of the dissemination of NMS hydrophone calibrations to end-users;

- increased scientific understanding of the physics of ultrasonic field measurement using hydrophones;
- potential in the future to widen the application of the model to different types of hydrophone.

It should be noted that whilst the project concentrated on developing a model for the only UK source of membrane hydrophones, the model could be applied to other membrane hydrophones, providing access is gained to the detailed physical characteristics of the devices that are essential if the model is to match particular devices.

2 PHASE 1: USER SURVEY AND LITERATURE REVIEW

2.1 GENERAL

Phase 1 represents the foundation of the information gathering exercise. This phase of the project has been undertaken using technical libraries and electronic search facilities available at NPL. The objective of this phase was to consider the different methods and their relative merits for the task in hand.

Information on user requirements has been gathered through a survey aimed at ensuring the development of the model and its capabilities closely meet the needs of the users. In order to provide a framework for this activity, an initial User Specification was prepared that defines the inputs and outputs of the model. This specification was in the form of a ‘Check List’, preceded by a minimum number of general questions. The questions asked cover:-

- the type of medical ultrasonic field being measured;
- the accuracies required for the different acoustical quantities;
- the available hydrophone/amplifiers and measuring systems;
- existing models used and their limitations;
- the type and importance of the different ‘input/outputs’ which could be provided in the model.

The survey involved approaching individuals in the following main groups:-

- hydrophone manufacturers and suppliers;
- key customers of hydrophone suppliers;
- medical ultrasonic equipment manufacturers;
- medical physics departments;
- standards and regulatory authorities.

2.2 USER SURVEY

A restricted report has been produced summarising the survey and outlining the findings.

The questionnaire, shown in Annex A, comprised six questions and was distributed to 30 recipients by PA using e-mail during August 2000. The mid-August deadline mentioned in the project proposal was slightly extended to allow for more replies.

Sixteen replies were received in total, constituting a yield of 53%. This represents a good outcome for an exercise of this type.

An initial analysis indicates that there is a strong interest in the project. Only one reply stated that a hydrophone model was already being used and only one organisation claimed to have no need for a hydrophone model. Accuracy requirements for the estimate of the acoustic pressure quantities were in the range of 2% to 20%. The fact that 25 μm pvdf, 0.5 mm diameter bilaminar hydrophones are widely used was confirmed, although these are used in conjunction with different types of loads: various types of oscilloscopes and amplifiers are listed in the replies which have been received. 87.5% of the users who replied use an amplifier of some description. More details can be found in Annex B. For reasons of confidentiality, names have been omitted and the replies grouped by country.

2.3 LITERATURE REVIEW

Literature searches have been completed and a summary of the findings is given here. The aim was to identify some of the methods that have been used to model the thickness mode of a piezoelectric transducer as well as attempts to model the transfer characteristics of hydrophones/transducers. Note that techniques involving two-dimensional wave propagation as well as finite element methods have not been included since they are beyond the scope of the original proposal.

Electroacoustic devices are often represented by equivalent electrical circuits. When a device may be represented by a circuit containing only lumped parameters (i.e. when the only independent variable is time), acoustical and mechanical quantities may be converted to electrical quantities via lumped parameter analogies. This allows electroacoustic devices to be analysed using electrical network concepts. Hence, using the equations of motion as well as the piezoelectric equations, expressions for equivalent electrical components may be derived and the equivalent circuit formed (12). There are generally two types of electrical equivalent circuit representations (13):

- The impedance analogue, where the velocity and force are respectively represented by the current and voltage.
- The mobility analogue, where the velocity and force are respectively represented by the voltage and current.

Electrical equivalent circuit methods have been used extensively to model the thickness mode of a piezoelectric transducer in both receiving and transmitting modes. Examples include:

- Transmission line analogies (14).
- Thévenin electrical circuits (15).

Other methods involve looking at the incident and reflected particle displacement wave within the piezoelectric element resulting from a given stress on the element when the latter is surrounded by two semi-infinite media (16) and is connected to an electrical load. The voltage produced across the element for an incident force is then evaluated. This approach has also been reformulated into a systems model in order to provide a better representation of the physics of the transduction process (17).

It should be noted that all of the above approaches are equivalent provided the system of equations describing the transducer system is the same. Also, the way in which these methods have been presented does not account for a multi-layered structure. A hydrophone may consist of several contiguous layers of piezoelectric (pvdf) and non-piezoelectric (gold, chromium) materials. Clearly, if an accurate model is to be developed, one must have a more general method for coping with a multi-layered structure.

In order to validate membrane hydrophone calibrations, a theoretical model describing the acoustic and electrical properties of the hydrophone has been developed by Koch and Molkenstruck (18). This model is based on an acoustic transmission-line formulation for a water-gold-pvdf-gold-water assembly. By knowledge of the piezoelectric and dielectric properties, an equivalent voltage source is derived. This source is then connected to an electric network comprising the lossy capacitances of the element and of water, an electrical transmission-line which models the hydrophone cable and an arbitrary electrical load. Although attention is paid to accurately characterise the electrical network, secondary piezoelectric effects are unaccounted for.

A computation technique for one-dimensional piezoelectric transducers, resonators or interferometers having an arbitrary number of layers and piezoelectric elements electrically in parallel has been derived using an electrical transmission line analogy (19). Expressions may be derived for the particle velocities and electrical impedances. Obtaining the transfer characteristics of a hydrophone consisting of an assembly of contiguous layers is therefore possible through use of this method.

Recognising the limitations of existing models for modelling arbitrary connections of transducers and/or acoustic and electrical loads, a new method of formulating the core matrix of a transducer model has been developed (20). This is done in the form of a translation matrix relating force and particle velocity on either side of the layer to the voltage and current associated with that layer. Coplanar and bilaminar hydrophones may be modelled using this technique and their transfer characteristics thus obtained.

This literature review outlines the fact that, as far as one-dimensional propagation is concerned, the fundamental equations describing the behaviour of a piezoelectric or non-piezoelectric layer of material form the starting point of each analysis. It is therefore a case of using a formulation that efficiently models an arbitrary configuration of layers. Although the method described in (20) would be adequate, a transfer matrix formulation has been chosen since prior modelling using this technique had already been attempted. This formulation is explained in detail in Section 3.2.2.

3 PHASE 2: DEVELOPMENT OF MODEL

3.1 GENERAL

The development and validation of the model involved:-

- finalising the details of the theoretical approach;
- preparation of the User and Functional Specifications for the model;
- writing and validating the core model software;
- establishment of reference data;
- technical validation.

Although the initial proposal to the DTI NMSPU included the writing and validating of user interface software, the option for an elaborate user interface was not taken up and only a basic type has been opted for.

3.2 ENVISAGED STRUCTURE OF THE MODEL

3.2.1 Modifications to initial proposal

The development of the model involved determining the overall acoustical to electrical transfer characteristics for the hydrophone and amplifier configuration. This includes four main elements:-

- acoustical;
- electrical on hydrophone;
- cable;
- amplifier.

The aim was to develop a model which would have wide future applicability whilst for this project concentrating on modelling the 'gold standard' membrane hydrophones most widely used in industry, the health services and universities.

- Due to Marconi not being involved in the project, many of the physical input data could not be measured as originally planned. Only the piezoelectric coefficient relating to the longitudinal part of the membrane deformation d_{33} was considered, and an approximate value was taken from the literature (21). The modulus of the relative permittivity was measured by PA on a failed 25 μm device between 1 MHz and 60 MHz. It was unfortunately impossible to measure the loss tangent, due to experimental difficulties, and values from literature had to be obtained (see Section 3.2.3).

- The geometrical sizes of the active element legs as well as the electrical leg resistance were measured by PA. The preparation of reference samples and the examination of manufacturing tolerances were unfortunately not possible. Estimates of the latter were produced, based mainly on the experience of the project team. The transfer characteristics of the leg had to be determined by knowledge of its DC resistance, its geometry, the relative permittivity as well as some theoretical considerations. The thickness of the electrodes was obtained from the literature.

- A sensitivity analysis was undertaken to examine the variation in overall transfer characteristics for variation in input data.

- The preparation of two reference hydrophones (9 and 25 μm) with accurately known characteristics was not possible. Instead, calibration data on 25 μm film thickness 0.5 mm diameter bilaminar hydrophones obtained from (22) was used to provide a technical validation of the model.

3.2.2 Theory

The aim of this section is to outline the theory used to compute the frequency response of a hydrophone consisting of *n* layers of material when placed in a given medium. It will be shown that if one-dimensional propagation is assumed, the transfer characteristics between the incident pressure at the front face of the hydrophone and the voltage across a piezoelectric layer may be deduced once the transfer matrices relating acoustic pressure and normal particle velocity on either side of each layer are determined. When the layer is made of a piezoelectric material, the terms of the transfer matrix associated with this layer will be a function of the electrical properties of the material as well as those of the equivalent electrical network that it is connected to. This electrical network will be characterised in the case of a bilaminar-shielded hydrophone and will be represented by a two-port network. When an electrical load is connected across the output terminals of this two-port network, the complete transfer characteristics of the hydrophone are defined as the voltage across this load for a unit incident pressure wave at the front face of the hydrophone.

3.2.2.1 Acoustical transfer characteristics

A. Reflection coefficient

Consider a hydrophone consisting of n-2 layers where the top-most and bottom-most layers are in contact with a specific medium. It is assumed that only plane-waves are normally incident on the surface of the top-most layer. Let x be the direction for normal propagation. Let p_i and u_{xi}, where $1 \leq i \leq n-1$, be the pressure and normal component of the particle velocity respectively at the top of the i^{th} layer, where i=1 corresponds to the top of the backing medium (see Figure 3.1).

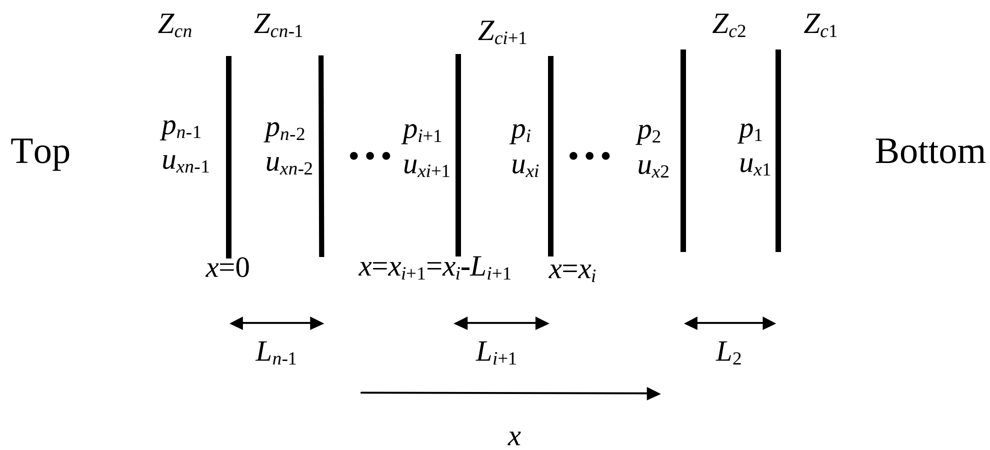

Figure 3.1: Schematic representation of a structure consisting of n-2 layers

Z_{ci} and L_i are respectively the characteristic impedance of the medium and the thickness corresponding to the i^{th} layer. Note that L_1 and L_n are not defined since these are associated with semi-infinite media on either side of the hydrophone.

Note that a coplanar or bilaminar hydrophone will contain layers of piezoelectric (pvdf) and non-piezoelectric (e.g. gold electrodes) materials.

It is of interest to be able to determine the pressure reflection coefficient of the transducer for a normally incident plane-wave on the top-most layer.

The pressure at the top-most layer will consist of an incident and reflected component:

$$p_{n-1} = \left(A_{n-1} e^{-jk_n x_{n-1}} + B_{n-1} e^{jk_n x_{n-1}} \right) e^{jwt} \quad (1)$$

where k_n is the complex wave number associated with the medium, x_i is the value of the x coordinate at the top of the i^{th} layer and w is the angular frequency.

The normal particle velocity at the top-most layer is given by:

$$u_{xn-1} = -\frac{1}{jwr_n} \frac{\P}{\P x} p_{n-1} = \frac{1}{Z_{cn}} \left(A_{n-1} e^{-jk_n x_{n-1}} - B_{n-1} e^{jk_n x_{n-1}} \right) e^{jwt} \quad (2)$$

where r_n is the density of the medium and Z_{cn} is the characteristic impedance of the medium ($Z_{cn}=r_n c_n$, where c_n is the velocity of sound in the medium).

The pressure reflection coefficient is defined as:

$$R = \frac{B_n}{A_n} \quad (3)$$

From equations (1), (2) and (3), it may be shown that:

$$R = \frac{Z_{sn-1} - Z_{cn}}{Z_{sn-1} + Z_{cn}} \quad (4)$$

where $Z_{sn-1} = p_{n-1}/u_{xn-1}$ is the surface impedance of the top-most layer.

Note that the absorption coefficient is defined as:

$$a = 1 - |R|^2 \quad (5)$$

Hence, it can be seen that if the surface impedance of the hydrophone can be determined, so can the pressure reflection coefficient. Once the transfer matrices for each layer of material have been characterised, it will be seen how the surface impedance and reflection coefficient can be used to obtain the hydrophone frequency response.

B. Transfer matrix of a non-piezoelectric layer

Consider now the pressure and normal particle velocity at the top of layer i.

$$p_i = \left(A_i e^{-jk_{i+1} x_i} + B_i e^{jk_{i+1} x_i} \right) e^{jwt} \quad (6)$$

$$u_{xi} = \frac{1}{Z_{ci+1}} \left(A_i e^{-jk_{i+1} x_i} - B_i e^{jk_{i+1} x_i} \right) e^{jwt} \quad (7)$$

By combining equations (6) and (7), the following expressions may be obtained:

$$A_i = \frac{1}{2}\left(p_i + Z_{ci+1}u_i\right)e^{jk_{i+1}x_i} \quad (8)$$

$$B_i = \frac{1}{2}\left(p_i - Z_{ci+1}u_i\right)e^{-jk_{i+1}x_i} \quad (9)$$

Consider now the pressure and normal particle velocity at the top of layer i+1. From pressure continuity, we have:

$$p_{i+1} = \left(A_{i+1}e^{-jk_{i+2}x_{i+1}} + B_{i+1}e^{jk_{i+2}x_{i+1}}\right)e^{jwt} = \left(A_i e^{-jk_{i+1}(x_i - L_{i+1})} + B_i e^{jk_{i+1}(x_i - L_{i+1})}\right)e^{jwt} \quad (10)$$

and from continuity of particle velocity:

$$u_{xi+1} = \frac{1}{Z_{ci+2}}\left(A_{i+1}e^{-jk_{i+2}x_{i+1}} - B_{i+1}e^{jk_{i+2}x_{i+1}}\right)e^{jwt} = \frac{1}{Z_{ci+1}}\left(A_i e^{-jk_{i+1}(x_i - L_{i+1})} - B_i e^{jk_{i+1}(x_i - L_{i+1})}\right)e^{jwt} \quad (11)$$

By substituting equations (8) and (9) into equations (10) and (11), the following matrix equation may be obtained:

$$\begin{Bmatrix} p_{i+1} \\ u_{xi+1} \end{Bmatrix} = \begin{bmatrix} \cos(k_{i+1}L_{i+1}) & jZ_{ci+1}\sin(k_{i+1}L_{i+1}) \\ \dfrac{j}{Z_{ci+1}}\sin(k_{i+1}L_{i+1}) & \cos(k_{i+1}L_{i+1}) \end{bmatrix} \begin{Bmatrix} p_i \\ u_{xi} \end{Bmatrix} \quad (12)$$

or

$$\begin{Bmatrix} p_{i+1} \\ u_{xi+1} \end{Bmatrix} = \left[T_{i+1}\right] \begin{Bmatrix} p_i \\ u_{xi} \end{Bmatrix} \quad (13)$$

where $[T_{i+1}]$ is the transfer matrix of the i+1th layer.

C. Transfer matrix of a piezoelectric layer

Consider a layer of piezoelectric material of thickness L subject to plane-wave incidence along the x-direction. Mechanical and electrical quantities such as displacement, stress and electrical field will therefore vary only in the x-direction (i.e. normal to the surface of the piezoelectric layer). In this case, the piezoelectric equations, as given by reference (17) are as follows:

$$\begin{aligned} \Gamma_x &= Y_x^D S_x - h_{33} D_x \\ E_x &= -h_{33} S_x + \frac{D_x}{e_x^S} \end{aligned} \quad (14)$$

where

- Γ is the stress (N m^{-2})
- S is the strain
- D is the electrical displacement (C m^{-2})
- E is the electrical field (V m^{-1})
- Y^D is the elastic constant measured under conditions of constant electrical displacement (N m^{-2})
- e^S is the permittivity measured under conditions of constant strain (F m^{-1})
- h_{33} is the piezoelectric constant (N C^{-1} or V m^{-1})

The *x* suffix refers to the fact that these quantities vary along the *x*-direction. Since no variations are assumed along the *y* and *z* axes, this suffix will be omitted.

By definition,

$$S = \frac{\partial x}{\partial x} \tag{15}$$

where *x* is the particle displacement.

In this case, Y^D corresponds to Young's Modulus.

When the piezoelectric element is subject to an incident plane pressure wave, it is clear that the stress is directly related to the acoustic pressure. It turns out that the sign convention adopted in equations (14) assumes that a positive stress results in a positive strain. This implies that the positive orientation for the stress is in the direction opposite to that for positive displacement. Hence, the acoustic pressure *p* is -Γ and

$$p = -Y^D S + h_{33} D \tag{16}$$

Applying Newton's second law of motion to an infinitesimal particle in the medium yields:

$$r\,\frac{\partial^2 x}{\partial x^2} = -\frac{\partial p}{\partial x} \tag{17}$$

From Gauss' law, since there is no free charge inside the piezoelectric material:

$$\vec{\nabla}.\vec{D} = 0 \tag{18}$$

where

$$\vec{\nabla} = \frac{\partial}{\partial x}\vec{x} + \frac{\partial}{\partial y}\vec{y} + \frac{\partial}{\partial z}\vec{z} \tag{19}$$

Since *D* only varies with *x*, equation (18) becomes:

$$\frac{\partial D}{\partial x} = 0 \tag{20}$$

Combining equations (16), (17) and (20) yields:

$$\frac{\partial^2 \hat{u}_x(x)}{\partial x^2} = -\frac{w^2}{c^2}\hat{u}_x(x) \tag{21}$$

where

- $u_x(x,t) = \dfrac{\partial x(x,t)}{\partial t}$ is the particle velocity along the *x*-axis
- $c^2 = Y^D/r$ where *c* is the speed of sound in the piezoelectric medium

- $u_x(x,t) = \hat{u}_x(x)e^{jwt}$

The solutions to equation (21) are of the form:

$$\hat{u}_x(x) = A_1 e^{-jkx} + B_1 e^{jkx} \tag{22}$$

where $k = w/c$ is the wave number.

As A_1 and B_1 are arbitrary constants, (22) may be rewritten as follows:

$$\hat{u}_x(x) = \frac{1}{rc}\left(Ae^{-jkx} - Be^{jkx}\right) \tag{23}$$

The acoustic pressure may be obtained from (16)

$$\hat{p}(x) = -\frac{rc^2}{jw}\frac{\partial \hat{u}_x(x)}{\partial x} + h_{33}D \tag{24}$$

Applying Gauss' law to the piezoelectric element leads to $D=Q/S$ at $x=0$ and $x=L$ where S is redefined as the surface area of the piezoelectric layer. This is true throughout the element since $\partial D/\partial x = 0$ (20). Hence, equations (23) and (24) may be rearranged as follows:

$$p(x,t) = \left(Ae^{-jkx} + Be^{jkx} + \frac{h_{33}Q}{S}\right)e^{jwt} \tag{25}$$

$$u_x(x,t) = \frac{1}{Z_c}\left(Ae^{-jkx} - Be^{jkx}\right)e^{jwt} \tag{26}$$

where $Z_c = rc$.

If the piezoelectric layer constitutes the i^{th} layer in a multi-layered structure as described in Section 3.2.2.1, the pressure and particle velocity at the top of this layer will therefore be given by:

$$p_i = \left(A_i e^{-jk_{i+1}x_i} + B_i e^{jk_{i+1}x_i} + \frac{h_{33}Q}{S}\right)e^{jwt} \tag{27}$$

$$u_{xi} = \frac{1}{Z_{ci+1}}\left(A_i e^{-jk_{i+1}x_i} - B_i e^{jk_{i+1}x_i}\right)e^{jwt} \tag{28}$$

These equations should be compared with equations (6) and (7).

As in Section 3.2.2.1.B, it is of interest to obtain the transfer matrix relating acoustic pressures and particle velocities on either side of the layer. Using a similar approach (i.e. making use of continuity of acoustic pressure and particle velocity between two contiguous layers), equations (27) and (28) can be shown to yield:

$$\begin{Bmatrix} p_{i+1} \\ u_{xi+1} \end{Bmatrix} = \begin{bmatrix} \cos(k_{i+1}L_{i+1}) & jZ_{ci+1}\sin(k_{i+1}L_{i+1}) \\ \frac{j}{Z_{ci+1}}\sin(k_{i+1}L_{i+1}) & \cos(k_{i+1}L_{i+1}) \end{bmatrix} \begin{Bmatrix} p_i \\ u_{xi} \end{Bmatrix} - \begin{Bmatrix} \frac{h_{33}Q}{S}\left[\cos(k_{i+1}L_{i+1}) - 1\right] \\ \frac{h_{33}Q}{S}\frac{j\sin(k_{i+1}L_{i+1})}{Z_{ci+1}} \end{Bmatrix} \tag{29}$$

If an electrical network of input impedance Z_E is connected to the electrodes of the piezoelectric layer, the voltage at the input stage of the network is given by (17):

$$V(w) = -h_{33}\left[x(x_i) - x(x_{i+1})\right] H(w) = -\frac{h_{33}}{jw}\left(u_{xi} - u_{xi+1}\right) H(w) \tag{30}$$

where

$$H(w) = \frac{Z_E}{Z_{el} + Z_E} \tag{31}$$

where Z_{el} is the impedance associated with the element capacitance C_{el}.

But Q is given by (17):

$$Q(w) = -\frac{V(w)}{jwZ_E} = \frac{h_{33}}{-w^2 Z_E}\left(u_{xi} - u_{xi+1}\right) H(w) \tag{32}$$

Hence, by substituting equation (32) into equation (29),

$$\begin{Bmatrix} p_{i+1} \\ u_{xi+1} \end{Bmatrix} = \begin{bmatrix} \cos(k_{i+1}L_{i+1}) & jZ_{ci+1}\sin(k_{i+1}L_{i+1}) \\ \dfrac{j}{Z_{ci+1}}\sin(k_{i+1}L_{i+1}) & \cos(k_{i+1}L_{i+1}) \end{bmatrix} \begin{Bmatrix} p_i \\ u_{xi} \end{Bmatrix} - \frac{h_{33}^2 H}{(jw)^2 Z_E S} \begin{Bmatrix} \left[\cos(k_{i+1}L_{i+1}) - 1\right](u_{xi} - u_{xi+1}) \\ \dfrac{j\sin(k_{i+1}L_{i+1})}{Z_{ci+1}}(u_{xi} - u_{xi+1}) \end{Bmatrix}$$

(33)

Define

$$a = \frac{h_{33}^2 H}{w^2 Z_E S}\left[\cos(k_{i+1}L_{i+1}) - 1\right] \tag{34}$$

$$b = \frac{h_{33}^2 H}{w^2 Z_E S}\frac{j\sin(k_{i+1}L_{i+1})}{Z_{ci+1}} \tag{35}$$

$$\begin{aligned} T_{i+1,11} &= \cos(k_{i+1}L_{i+1}) \\ T_{i+1,12} &= jZ_{ci+1}\sin(k_{i+1}L_{i+1}) \\ T_{i+1,21} &= \frac{j}{Z_{ci+1}}\sin(k_{i+1}L_{i+1}) \\ T_{i+1,22} &= \cos(k_{i+1}L_{i+1}) \end{aligned} \tag{36}$$

By rearranging equation (33), it may be shown that:

$$\begin{Bmatrix} p_{i+1} \\ u_{xi+1} \end{Bmatrix} = \begin{bmatrix} T_{i+1,11} - \dfrac{aT_{i+1,21}}{1+b} & T_{i+1,12} + \dfrac{a(1-T_{i+1,22})}{1+b} \\ \dfrac{T_{i+1,21}}{1+b} & \dfrac{T_{i+1,22}+b}{1+b} \end{bmatrix} \begin{Bmatrix} p_i \\ u_{xi} \end{Bmatrix} \tag{37}$$

It is easily shown that equation (37) is equivalent to equation (12) when Z_E tends to infinity (i.e. open-circuit case).

From (13) and (37), it follows that:

$$\begin{Bmatrix} p_{n-1} \\ u_{xn-1} \end{Bmatrix} = [T_{n-1}][T_{n-2}]\cdots[T_2]\begin{Bmatrix} p_1 \\ u_{x1} \end{Bmatrix} \tag{38}$$

where the transfer matrices may refer to either piezoelectric or non-piezoelectric layers. Hence coplanar as well as bilaminar hydrophones may be modelled.

Equation (38) is rewritten as follows.

$$\begin{Bmatrix} p_{n-1} \\ u_{xn-1} \end{Bmatrix} = [T]\begin{Bmatrix} p_1 \\ u_{x1} \end{Bmatrix} \tag{39}$$

where [T] is the transfer matrix associated with the hydrophone.

Note that p_1 is the pressure transmitted into the medium backing the hydrophone.

3.2.2.2 Electrical transfer characteristics

A. Transfer characteristics between the pressure at the front face of the hydrophone and the voltage across a layer of pvdf

Consider equations (13) and (37). If the expression for p_{i+1} is divided by that for u_{xi+1}, a recurring relationship between the surface impedances of two consecutive layers may be obtained:

$$Z_{si+1} = \frac{p_{i+1}}{u_{xi+1}} = \frac{Z_{si}T_{i,11} + T_{i,12}}{Z_{si}T_{i,21} + T_{i,22}} \tag{40}$$

where $Z_{si} = \dfrac{p_i}{u_{xi}}$.

The initial value Z_{s1} of the surface impedance is the value of the characteristic impedance of the backing medium. Hence, Z_{s1}=Z_{c1}. By knowledge of the characteristics of each layer of the hydrophone, it is therefore possible to obtain the surface impedance Z_{sn-1} at the top-most layer.

The pressure reflection coefficient R as well as the absorption coefficient a may then be evaluated using equations (4) and (5).

In order to evaluate the pressure transmission coefficient T, consider the total pressure and particle velocity at the top-most layer of the hydrophone (see equations 1 and 2). At the top-most layer, x=0. By making use of this and by dividing (1) by (2), the following equation may be obtained:

$$u_{xn-1} = \frac{p_{n-1}}{Z_{cn}}\left(\frac{1-R}{1+R}\right) \tag{41}$$

From equation (39), the transmitted pressure from the hydrophone into the medium may be obtained through inversion of the transfer matrix and by making use of equation (18):

$$p_1 = T_{11}^{-1} p_{n-1} + T_{12}^{-1} \frac{p_{n-1}}{Z_{cn}} \left(\frac{1-R}{1+R} \right) \tag{42}$$

where $[T]^{-1} = \begin{bmatrix} T_{11}^{-1} & T_{12}^{-1} \\ T_{21}^{-1} & T_{22}^{-1} \end{bmatrix}$

From equation (1), it is easily shown that the incident component of the pressure wave at the top-most layer is:

$$A_{n-1} = \frac{p_{n-1}}{1+R} \tag{43}$$

By definition, the pressure transmission coefficient T is the ratio of the transmitted pressure to the incident pressure or:

$$T = \frac{p_1}{A_{n-1}} = T_{11}^{-1}(1+R) + T_{12}^{-1} \frac{(1-R)}{Z_{cn}} \tag{44}$$

Although the transmission coefficient is not fundamental to the computation of the hydrophone transfer function, it is included here for the sake of completeness.

In order to determine the transfer characteristics between the pressure at the front face of the hydrophone and the voltage across a layer of pvdf, one must consider the Fourier transform of the voltage for a unit incident plane wave on the front face of the hydrophone. From equation (43), this implies that p_{n-1} = 1+R. u_{xn-1} can then be obtained by using equation (41). Hence, since the acoustic pressure and particle velocity at the top-most layer as well as the transfer matrices associated with each layer are known, the pressure and particle velocity at the top of any layer may be determined using equation (38). The voltage across piezoelectric layers may therefore be determined using equation (30).

B. Characteristics of the equivalent electrical network in the case of a bilaminar-shielded hydrophone

The type of bilaminar hydrophone to be modelled consists of two pvdf membranes separated by a live electrode, the outer surfaces of the pvdf being bonded to earth electrodes. The electrodes are made of gold and chromium is used to bond these onto the pvdf. The front pvdf membrane is joined to the rear via a nitrile rubber adhesive. From front to back the layers are therefore as follows:

gold-chromium- pvdf -adhesive-gold-chromium- pvdf -chromium-gold

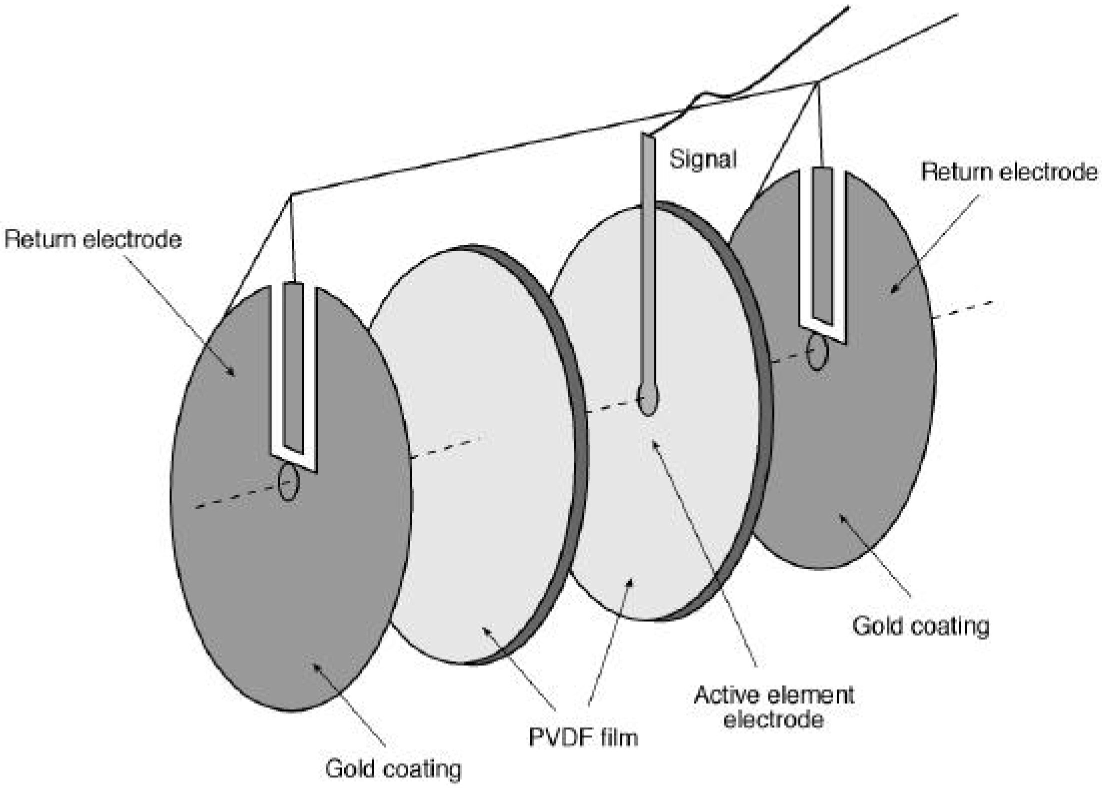

Figure 3.2: Diagram of a bilaminar membrane hydrophone.

As the piezoelectric active element undergoes compression and rarefaction resulting from an incident ultrasonic pressure wave, an electrical charge across each pvdf layer is generated which is converted into an electrical voltage by virtue of the inherent electrical capacitances. Hence, the pvdf membranes each behave as equivalent voltage sources in series with a capacitance.

V_1 and V_2 are respectively the voltages associated with the equivalent voltage sources of the front and rear pvdf layers.

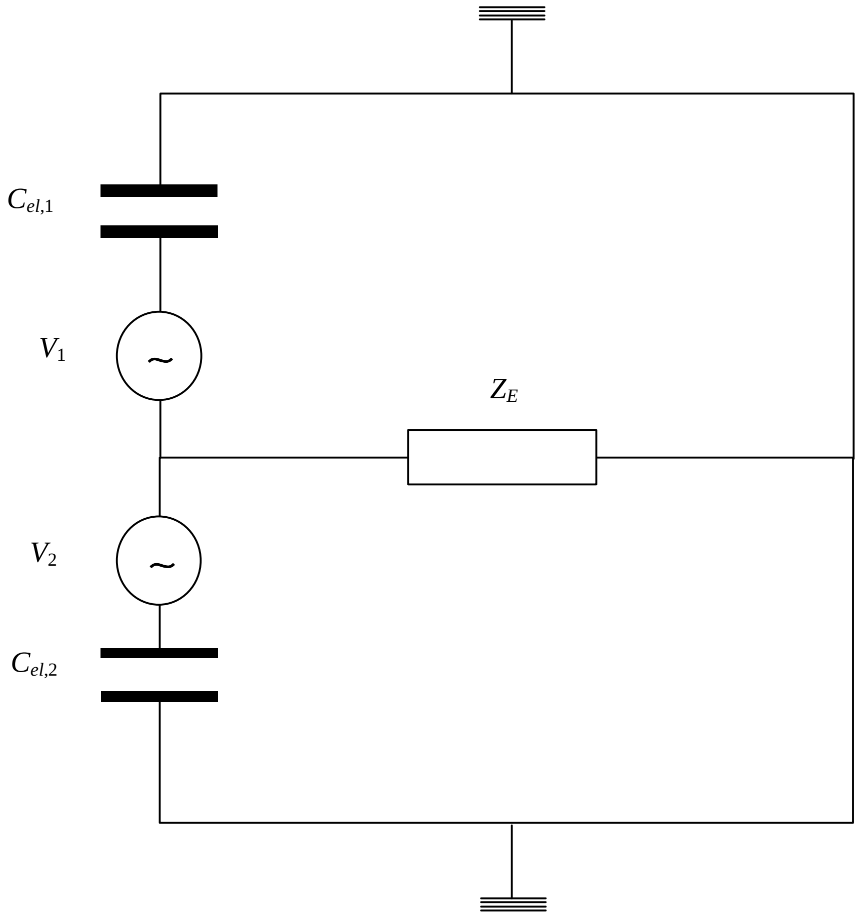

Figure 3.3 Electrical equivalent circuit of a bilaminar hydrophone in terms of the electrical input impedance Z_E of the network connected to the active element.

$C_{el,1}$ and $C_{el,2}$ are respectively the element capacitances associated with the front and rear pvdf layers. They are given by:

$$C_{el,i} = \frac{e_r e_0 S}{L_i} \tag{45}$$

where
- e_r is the relative permittivity of the pvdf film
- e_0 is the permittivity of free space
- S is the surface area of the active element
- L_i is the film thickness.
- i is 1 or 2.

In the case of an ideal device, $C_{el,1}$ and $C_{el,2}$ should be equal, but in practice, they may vary slightly from one another due to manufacturing tolerances (for example variations in pvdf thickness).

The relative permittivity e_r is in this case a complex quantity given by:

$$e_r = e_r'(1 - \tan d) \tag{46}$$

where
- e_r' is the real part of the relative permittivity of pvdf

- tan$d$ is the loss tangent of pvdf.

This effectively means that the element capacitances are lossy and the impedances $Z_{el,i}$ associated with these are not purely reactive and hence have a real part:

$$Z_{el,i} = \frac{1}{jw \frac{e_r e_0 S}{t_i} \left(1 - j \tan d\right)} \tag{47}$$

It is likely that there is a depoled region of thickness $L_{i,depoled}$ in each pvdf layer, located at the end of the layer which is closest to the rear of the hydrophone (23). This can in fact be modelled by including a separate layer of pvdf which is considered free of piezoelectric effects The poled layer is clearly of thickness L_i-$L_{i,depoled}$. Note that the thickness used for determining the capacitance is still L_i

Z_E is the input electrical impedance of the equivalent electrical network connected to the active element. The details of this network will be examined at a later stage. It will be assumed that Z_E has been characterised. The network in Figure 3.3 will be redrawn as follows (see Figure 3.4).

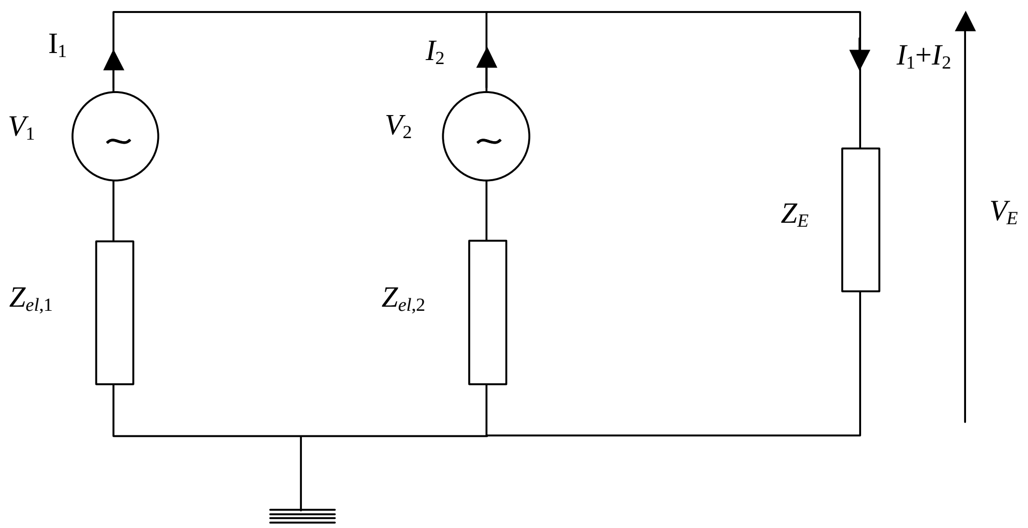

Figure 3.4: Other view of Figure 3.3.

From equation (3), it is easily shown that when the piezoelectric layer constitutes the i^{th} layer of a multi-layered structure, the voltage across the element is given by:

$$V(w) = -h_{33}\left[x(x_i) - x(x_{i+1})\right] = -\frac{h_{33}}{jw}\left(u_{xi} - u_{xi+1}\right) \tag{48}$$

When the element is connected to a network of input impedance $Z_{E,}$ the voltage at the input of this network is then given by equation (30).

In the case of a bilaminar hydrophone, it is found that the normal particle velocities on each side of a layer of pvdf will be dependent on the voltage across the other pvdf layer. Consider the transfer functions H_1 and H_2 defined as follows:

$$H_1 = \frac{V_E}{V_1} = \frac{(I_1 + I_2)Z_E}{\left(I_1 + I_2\right)Z_E + I_1 Z_{el,1}} \tag{49}$$

$$H_2 = \frac{V_E}{V_2} = \frac{(I_1 + I_2)Z_E}{(I_1 + I_2)Z_E + I_2 Z_{el,2}} \tag{50}$$

It is easily shown that:

$$I_1 = \frac{V_1 + (V_1 - V_2)\frac{Z_E}{Z_{el,2}}}{Z_E\left(1 + \frac{Z_{el,1}}{Z_{el,2}}\right) + Z_{el,1}} \tag{51}$$

$$I_2 = \frac{I_1 Z_{el,1} - (V_1 - V_2)}{Z_{el,2}} \tag{52}$$

Hence, by knowledge of the transfer functions H_1 and H_2 as a function of frequency, the transfer matrix associated with the pvdf layer can be characterised and it is possible to evaluate the acoustic pressures and normal particle velocities on either side of each pvdf layer by virtue of the transfer matrix method described in Section 3.2.2.1. In order to compute H_1 and $H_{2,}$ consider an iterative loop where secondary piezoelectric effects are initially neglected. a and b in equations (34) and (35) are therefore initially set to zero. The pvdf pressures and normal particle velocities, which no longer depend on the electrical network, are then computed. V_1 and V_2 can then be obtained using equation (48) and I_1, I_2, H_1 and H_2 may then be deduced. On the second iteration, a and b are set to their expressions in equations (34) and (35) whereby H is replaced by H_1 or H_2 (depending on which pvdf layer is being considered) and the process is repeated until convergence of V_E, the voltage across Z_E, is achieved.

The input impedance of the equivalent electrical network connected to the electrodes is to be determined in this section. The equivalent electrical network consists of two sections: the leg and the loaded coaxial cable. Each of these will be described and analysed.

C. Leg transfer characteristics

A bilaminar hydrophone has a leg connecting the active element to the periphery of the hydrophone. It is located on the inner surface of one of the pvdf sheets. The leg is a thin film of chromium overcoated with gold.

To a first order approximation, the leg may be modelled as a shunt lossy capacitance with a series resistance. The capacitance of the leg is dependent on the width of the coating and its length, the thickness of the pvdf layer and the dielectric constant. There are in fact two parallel-plate capacitances in parallel and the overall capacitance is given by:

$$C_{leg} = C_{leg,1} + C_{leg,2} = \frac{e_r e_0 w_{leg} L_{leg}}{t_1} + \frac{e_r e_0 w_{leg} L_{leg}}{t_2} \tag{54}$$

where
- w_{leg} is the width of the leg coating
- L_{leg} is the length of the leg
- t_1 and t_2 are the thicknesses of the pvdf layers

The leg resistance R_{leg} may be obtained from measurement.

In reality, the leg is best modelled as a ladder network containing distributed shunt capacitances and series resistors as shown in Figure 3.5.

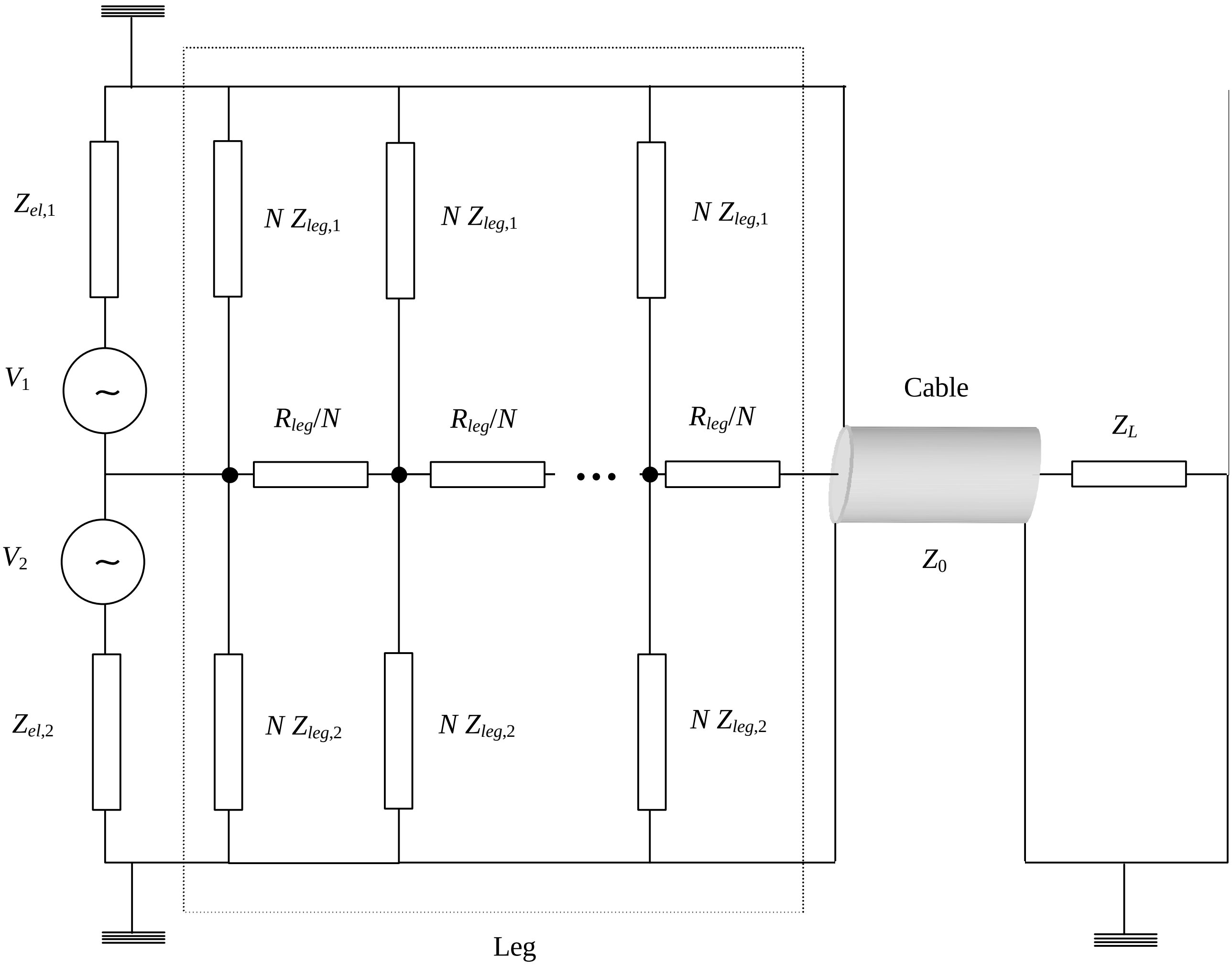

Figure 3.5: Equivalent electrical circuit of a bilaminar hydrophone showing the details of the leg network and the load cable.

N is the number of branches considered. The shunt capacitance in each branch is the total leg capacitance divided by the number of branches *N*. The series resistance in each branch is the total leg resistance divided by the number of branches *N*. The transfer characteristics for such a network may be obtained by considering the transfer matrix of a single branch which relates voltage and current at the input and output stages. Let $NZ_{leg,1}$ and $NZ_{leg,2}$ be the impedances associated with $C_{leg,1}/N$ and $C_{leg,2}/N$ in each branch. NZ_{leg} is then defined as the total shunt impedance in a single branch of the network. NZ_{leg} is the parallel combination of $NZ_{leg,1}$ and $NZ_{leg,2}$. See Figure 3.6.

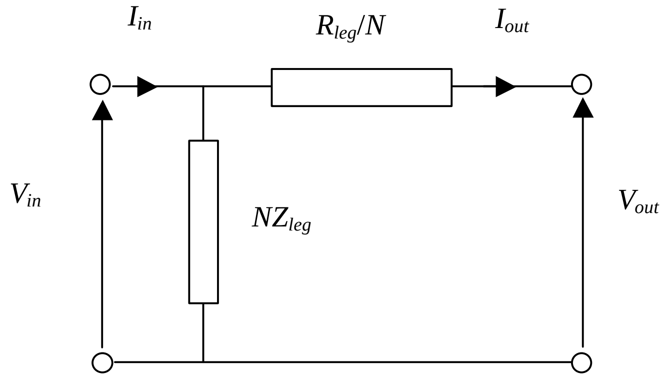

Figure 3.6: Figure of a single branch of the leg network.

It is easily shown that:

$$\begin{Bmatrix} V_{in} \\ I_{in} \end{Bmatrix} = \begin{bmatrix} 1 & \dfrac{R_{leg}}{N} \\ \dfrac{1}{NZ_{leg}} & \dfrac{\dfrac{R_{leg}}{N} + NZ_{leg}}{NZ_{leg}} \end{bmatrix} \begin{Bmatrix} V_{out} \\ I_{out} \end{Bmatrix} \tag{55}$$

$$[T_{leg,branch}] = \begin{bmatrix} 1 & \dfrac{R_{leg}}{N} \\ \dfrac{1}{NZ_{leg}} & \dfrac{\dfrac{R_{leg}}{N} + NZ_{leg}}{NZ_{leg}} \end{bmatrix} \tag{56}$$

$[T_{leg,branch}]$ is the transfer matrix of a single branch of the leg network. If the network contains N branches, the complete transfer matrix is given by:

$$[T_{leg}] = [T_{leg,branch}]^N = \begin{bmatrix} A_{leg} & B_{leg} \\ C_{leg} & D_{leg} \end{bmatrix} \tag{57}$$

In reality, $N \rightarrow \infty$, but a good approximation can be obtained by taking N of the order of 10^2.

D. Coaxial cable transfer characteristics

The leg is connected to a coaxial cable so that the hydrophone may be connected to an amplifier or oscilloscope. In order to model the transfer characteristics of the loaded coaxial cable, a transfer matrix approach will once again be adopted. This allows the determination of the loaded cable input impedance as well as the leg input impedance.

Consider the equations for the voltage V_{cable} and the current I_{cable} at a distance x inside the cable (18):

$$V_{cable} = V_{cable,1} e^{-jbx} + V_{cable,2} e^{jbx} \tag{58}$$

$$I_{cable} = \frac{1}{Z_0}\left(V_{cable,1}e^{-jbx} - V_{cable,2}e^{jbx}\right) \tag{59}$$

where

- $V_{cable,1}$ and $V_{cable,2}$ are cable constants which depend on the boundary conditions
- $b = w/c_{cable}$ is the propagation constant of the cable (c_{cable}=2×10^8 m s^{-1} is the propagation speed)
- Z_0 is the cable characteristic impedance.

Assume that x=0 at the front end of the cable and x=l_{cable} at the back end of the cable, where l_{cable} is the cable length.

At x=0, the cable input voltage $V_{cable,in}$ and current $I_{cable,in}$ are:

$$V_{cable} = V_{cable,1} + V_{cable,2} = V_{cable,in} \tag{60}$$

and

$$I_{cable} = \frac{1}{Z_0}\left(V_{cable,1} - V_{cable,2}\right) = I_{cable,in} \tag{61}$$

At x=l_{cable}, the cable input voltage $V_{cable,out}$ and current $I_{cable,out}$ are:

$$V_{cable} = V_{cable,1}e^{-jb\,l_{cable}} + V_{cable,2}e^{jb\,l_{cable}} = V_{cable,out} \tag{62}$$

and

$$I_{cable} = \frac{1}{Z_0}\left(V_{cable,1}e^{-jb\,l_{cable}} - V_{cable,2}e^{jb\,l_{cable}}\right) = I_{cable,out} \tag{63}$$

By eliminating the cable constants, in equations (60) to (63), it can be shown that:

$$\begin{Bmatrix} V_{cable,in} \\ I_{cable,in} \end{Bmatrix} = \begin{bmatrix} \cos(ab\,l_{cable}) & jZ_0\sin(b\,l_{cable}) \\ \dfrac{j\sin(b\,l_{cable})}{Z_0} & \cos(b\,l_{cable}) \end{bmatrix} \begin{Bmatrix} V_{cable,out} \\ I_{cable,out} \end{Bmatrix} \tag{64}$$

and the transfer matrix associated with the cable is:

$$\left[T_{cable}\right] = \begin{bmatrix} \cos(b\,l_{cable}) & jZ_0\sin(b\,l_{cable}) \\ \dfrac{j\sin(b\,l_{cable})}{Z_0} & \cos(b\,l_{cable}) \end{bmatrix} \tag{65}$$

When the cable is connected to an electrical load of impedance Z_L,

$$Z_L = \frac{V_{cable,out}}{I_{cable,out}} \tag{66}$$

The input impedance of the cable is then given by:

$$Z_{cable,in} = \frac{Z_L \cos(b\,l_{cable}) + jZ_0 \sin(b\,l_{cable})}{j\frac{Z_L}{Z_0}\sin(b\,l_{cable}) + \cos(b\,l_{cable})} \tag{67}$$

In the case of an open circuit cable termination, $Z_L \to \infty$ and

$$Z_{cable,in} = \frac{Z_0}{j\tan(b\,l_{cable})} \tag{68}$$

E. Electrical impedance Z_E seen by the active element

The backing impedance seen by the leg is the input impedance of the loaded cable $Z_{cable,in}$ and the input impedance of the leg $Z_{leg,in}$ which is also Z_E is given by:

$$Z_E = Z_{leg,in} = \frac{A_{leg} Z_{cable,in} + B_{leg}}{C_{leg} Z_{cable,in} + D_{leg}} \tag{69}$$

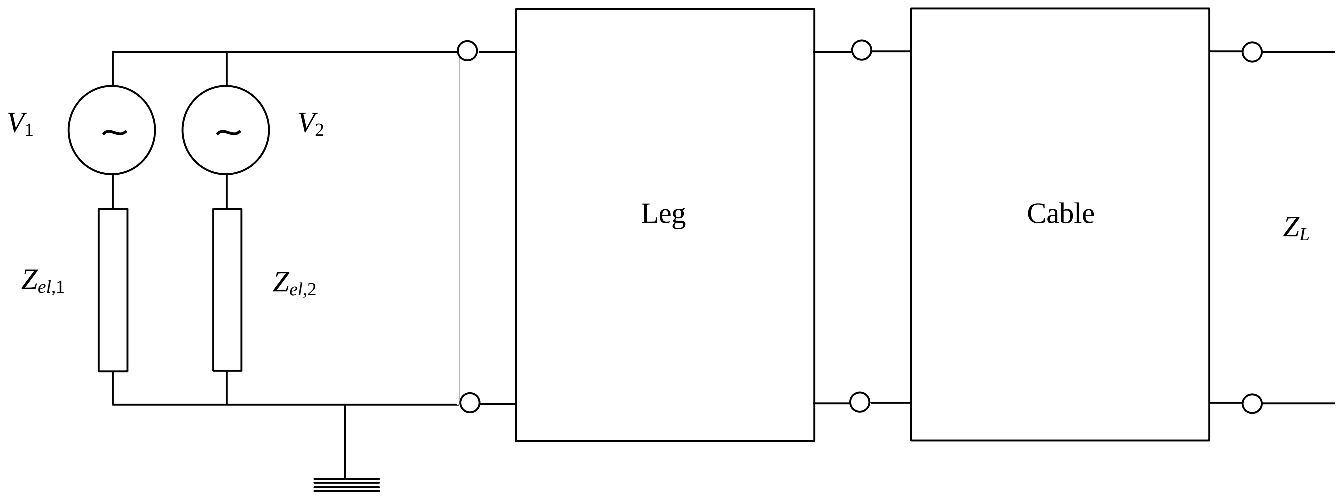

Figure 3.7: Two-port network representation of the leg and coaxial cable.

Once Z_E is determined as a function of frequency, this enables the calculation of the voltage V_E at the input of the leg as a function of frequency by use of the iteration procedure described in Section 3.2.2.2.B. The current I_E entering the leg is simply I_1+I_2 (see Section 3.2.2.2.B).

F. Complete transfer characteristics and amplifier transfer

The complete transfer characteristics of the bilaminar hydrophone are defined as the output voltage V_L across the load of impedance Z_L at the cable termination for a normally incident unit plane pressure wave at the front face of the hydrophone.

We have: Z_L

$$\begin{Bmatrix} V_E \\ I_E \end{Bmatrix} = \left[T_{leg}\right]\left[T_{cable}\right]\begin{Bmatrix} V_L \\ I_L \end{Bmatrix} \tag{70}$$

As V_E, I_E, $[T_{leg}]$ and $[T_{cable}]$ are all known, the values of V_L and I_L may be obtained by performing a matrix inversion at each frequency.

$$\begin{Bmatrix} V_L \\ I_L \end{Bmatrix} = \left([T_{leg}][T_{cable}]\right)^{-1} \begin{Bmatrix} V_E \\ I_E \end{Bmatrix} \tag{71}$$

Although determining I_L as a function of frequency is not essential, the ratio V_L/I_L may be compared against the assigned value of the load Z_L to make sure that these match.

In order to account for the presence of the amplifier, an ideal case will be considered instead of a two-port network analysis. It is assumed that the amplifier draws minimal current and is a voltage controlled device of complex gain $G(w)$. This gain is to include the transfer characteristics of any network following the amplifier. When the amplifier is connected to the cable termination, the latter effectively "sees" the input impedance of the amplifier. The voltage V_{out} at the output stage of the electrical network connected to the amplifier is simply:

$$V_{amp,out}(w) = V_L(w)G(w) \tag{72}$$

where V_L is obtained by knowledge of the amplifier's input impedance, which is effectively the load impedance Z_L.

3.2.3 Acquisition of base membrane hydrophone data

3.2.3.1 Constructional data background

Accurate modelling of the performance of the bilaminar membrane hydrophone requires assessment of a range of parameters relating to the construction and geometry of the device. Many of these parameters are not readily measurable. Fortunately, the project team had access to a range of historical data for values and tolerances of these parameters. A summary of this information is provided in Table 3.1 below.

Parameter	Mean value	Typical tolerance
Electrode leg length (mm)	56.5	± 1.5
Electrode leg width (μm)	200	± 5
Thickness of evaporated chrome (nm)	50	± 25
Thickness of evaporated gold (nm)	100	± 50
pvdf film thickness (μm)	25	± 2
Diameter of active element (μm)	500	± 5

Table 3.1: Construction properties of membrane hydrophones

3.2.3.2 Electrode leg resistance

A. Background

The construction of a membrane hydrophone requires that an electrode connection is made to the hydrophone active element. The active element electrode and thus the electrode leg are found between the two layers of pvdf that go to make a bilaminar membrane hydrophone. Due to the limited dimensions of the gold layer that comprises the electrode leg, there will be an associated finite resistance.

B. Procedure

To be able to measure the resistance of the electrode leg, it is necessary to gain access to either end of it. As described above, the electrode is between the two laminated layers of pvdf of a bilaminar hydrophone. The membrane hydrophone was placed under a high power optical microscope. An area of the outer layer of pvdf, slightly to one side of the active element, was carefully cut away with a scalpel. Then a scalpel and tweezers were used to separate the two laminated layers of the membrane. This procedure was continued until the active electrode was fully exposed.

By resting the membrane on a solid but rubbery surface, a good pressure contact could be made between the probe of an impedance meter and the exposed electrode. The connection to the other end of the electrode was made via the core of the co-axial cable. Thus measurements of leg resistance also include the resistance of the conductive epoxy connection between cable core and leg electrode. DC resistance was measured using a simple digital multi-meter.

C. Results

Measurement of DC resistance by the method described above seemed to yield very consistent results. Ten individual measurements were taken to yield the following results:

- mean DC resistance = 142.2 Ω
- standard deviation = 0.4 Ω

Total uncertainty (systematic + random) = ± 5% on this measurement but in general there could be greater variation between individual devices due to variations in the thickness of the gold layer.

An estimation of leg impedance can be made as follows:

Area of leg electrode = 0.2 mm × 50 mm = 25 mm^2
Approximate surface resistance for a good (2000 Å thick) gold electrode = 5 Ω/mm^2
Estimated Resistance = 5 × 25 = 125 Ω

This estimated value is consistent with the experimentally determined value of DC Resistance for the leg electrode.

3.2.3.3 Dielectric constant of pvdf film

A. Background

An important factor affecting the electrical performance of a pvdf sensor is the capacitance that the material presents. The dielectric constant e_r (also known as relative permittivity) of a material can be derived from the parallel plate capacitor equation:

$$C = \frac{e_0 e_r A}{d} \quad (73)$$

where e_o is the permittivity of free space, *A* is the area of one of the capacitor plates, *d* is the parallel distance between the plates and *C* is the capacitance. The pvdf film as found in a membrane hydrophone is already metallised, and this conveniently serves as the capacitor plate.

B. Procedure

Three circular samples were cut from the membrane of a Marconi bilaminar hydrophone. Circular samples were used in preference to square samples in order to reduce the effects of field fringing that would be seen at the corner of a square sample. The key to a successful measurement of capacitance is to minimise additional inductances that are present, often in the form of conducting leads. To this end, an electrode was attached via conductive epoxy to one side of the pvdf film only. Initially the electrode length was of the order of 35 mm, but as experimentation proceeded this was reduced and the effect upon measured capacitance was observed. The final electrode length was of the order of 14 mm. However, once electrode length was less than 19 mm there was very little variation as further reductions in lead length were made.

A measurement of impedance for each of the samples was made using an HP8712C vector network analyser over the frequency range 1-60 MHz. Data points were recorded at 0.5 MHz intervals. From the imaginary component of impedance the capacitance was derived, and then equation (73) was used to finally obtain a value for dielectric constant for each of the samples. Theoretically, the real component of impedance could be used to derive the dielectric loss for each sample. However, the real components of the impedance were so small that they were dominated by the real resistance of the conductive epoxy that was used to affix the electrodes. This rendered an assessment of dielectric loss unattainable.

C. Results

The mean dielectric constant as a function of frequency can be found in Figure 3.8 below. The error bars indicate total (i.e. random + systematic) uncertainty.

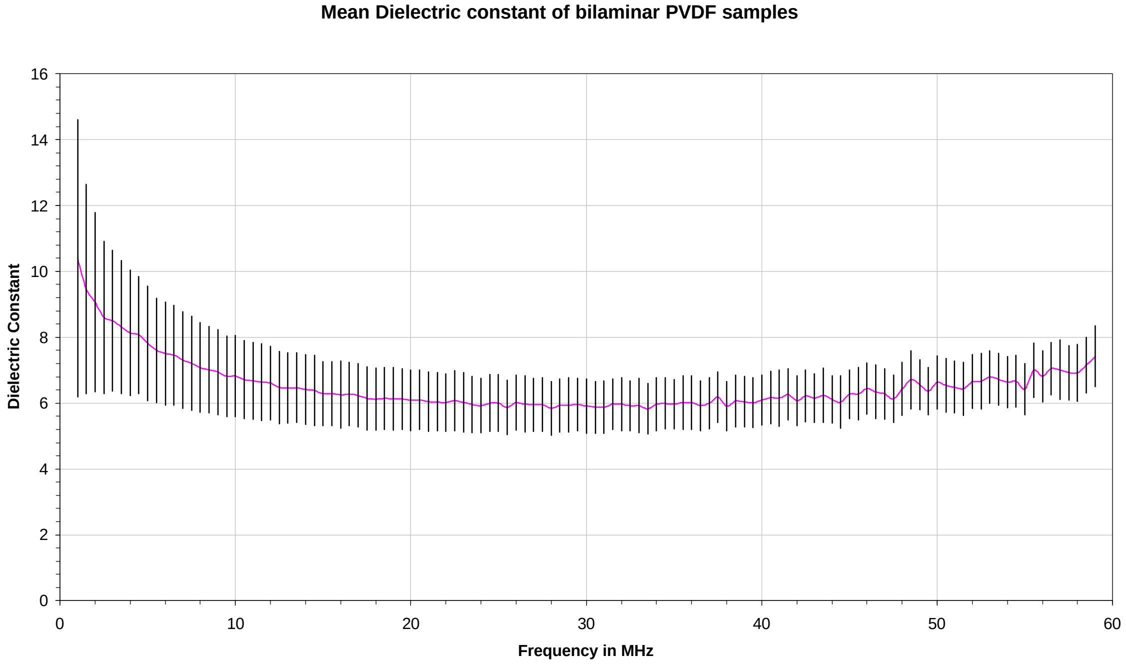

Figure 3.8: Mean value of the modulus of the relative permittivity of bilaminar pvdf samples.

Consider now the plot of the mean value of $|e_r|$ as a function of $\log_{10}(f)$, where f is the frequency in Hz, shown in Figure 3.9.

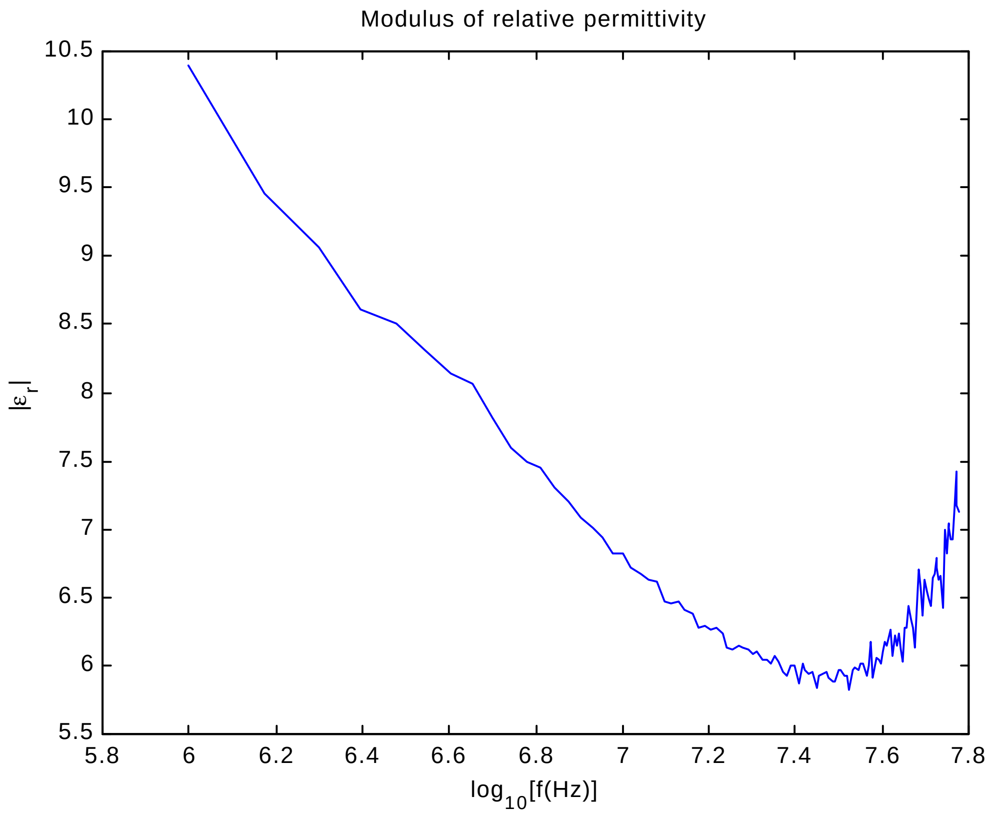

Figure 3.9: Mean value of the modulus of the relative permittivity of bilaminar pvdf samples plotted as a function of the decimal logarithm of the frequency.

More work would need to be done in order to validate the values obtained beyond $10^{7.4}$ Hz. Hence, in order to extend the range of frequencies over which the mean value of $|e_r|$ may be used, the same approach to that used as in (18) is employed here. A linear polynomial fit as a function of $\log_{10}(f)$, where f is the frequency in Hz, is done for frequencies between 10^6 and $10^{7.4}$ Hz:

$$|e_r| \approx -2.82\log_{10}\left[f\,(\mathrm{Hz})\right] + 26.7 \qquad (74)$$

3.3 VALIDATION

3.3.1 Comparison with measured data

As mentioned in Section 3.2.1, some of the work described in the original proposal could not be carried out. In order to validate the model, open circuit calibration data on 25 μm film thickness 0.5 mm diameter bilaminar hydrophones was obtained from (22).

The list of input parameters necessary to the implementation of the theory described in Section 3.2 is shown in Table 3.2. The data listed here applies to a 25 μm pvdf, 0.5 mm diameter shielded bilaminar hydrophone.

c: velocity of sound (m s^{-1})	water: 1482.36 (24); gold: 3240 (25); chromium: 6608 (25); pvdf: 2300 (6); glue: 1600 (26)*
r: material density (kg m^{-3})	water: 998.2 (27); gold: 19281 (28); chromium: 7194 (28); pvdf: 1780 (6); glue 1000*
t: thickness of layer (μm)	gold: 0.1; chromium: 0.05; pvdf (poled+depoled): 25; depoled pvdf region: 0.7** per membrane; glue: 0.5
a: attenuation coefficient (neper m^{-1} MHz^{-1})	pvdf: 111 (25); glue: 104 (26)*
d_{33}: piezoelectric coefficient (pC N^{-1})	15 (21)
e_0: dielectric constant (pF m^{-1})	8.85
$\|e_r\|$: modulus of relative permittivity of pvdf (as a function of frequency f in Hz)	$-2.82 \log_{10}(f)+26.7$ (linear fit to measurement; see Section 3.2.3)
tan d: loss tangent of relative permittivity of pvdf (as a function of frequency f in MHz)	$0.22 + 0.07 \log_{10}(f) - 0.055 \log_{10}(f)^2$ (18)
r: element radius (mm)	0.25
w_{leg}: leg width (mm)	0.2
l_{leg}: leg length (mm)	56.5
R_{leg}: leg resistance (Ω)	142 (obtained from measurement; see Section 3.2.3)
N: order of leg network	70
c_{cable}: velocity of wave propagation in cable (m s^{-1})	2×10^8 (18)
l_{cable}: length of cable (cm)	71 (18)
Z_0: cable characteristic impedance (Ω)	75 (18)

Table 3.2: List of model input parameters.

*: The Nitrile Rubber properties have been estimated by using the same sound speed and attenuation as that of rubber and a material density approximately equal to that of water.

**: The thickness of the depoled region is the same as that used in (18). Although there is not much justification for employing this value, it was found that agreement with experimental results was slightly improved. This feature is included in the model mainly for the sake of completeness.

Note that d_{33} is related to h_{33} via:

$$h_{33} = \frac{d_{33}\, r_{PVDF}\, c_{PVDF}^2}{e_0 e_r} \tag{75}$$

The predicted open circuit sensitivity is shown together with the thirteen calibrations obtained in (22) in Figure 3.10.

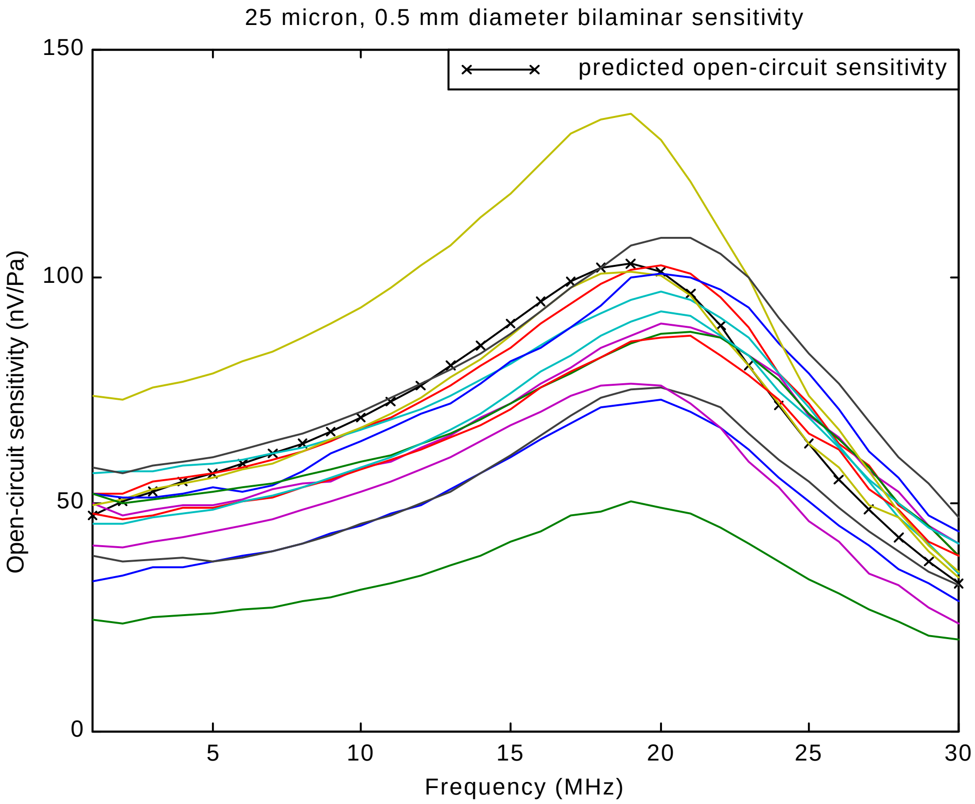

Figure 3.10: Sensitivities measured for thirteen nominally identical 25 micron, 0.5 mm bilaminar hydrophones (coloured plots) together with sensitivity predicted by model using the input data in Table 3.2.

It can be seen that the measured sensitivities span quite a large range. Other than the random and systematic errors resulting from the measurements, there will be some variations between the devices due to manufacturing tolerances. For example, it is likely that quantities such as the pvdf and gold thickness, the relative permittivity, the element and leg geometries may vary from one hydrophone to another. In the next section a sensitivity analysis will be carried out in which some of the input parameters in Table 3.2 will be varied within specific ranges.

3.3.2 Sensitivity analysis

The parameters in Table 3.3 have been chosen to be varied in the sensitivity analysis:

t: thickness of layer (μm)	gold: 0.1 ±0.05; chromium: 0.05 ±0.025; pvdf (poled+depoled): 25 ±2;
d_{33}: piezoelectric coefficient (pC N^{-1})	15 ±2.5
$\|e_r\|$: modulus of relative permittivity of pvdf (as a function of frequency f)	$\|e_r\| \pm 0.2\ \|e_r\|$
r: element radius (μm)	250 ±2.5
w_{leg}: leg width (μm) l_{leg}: leg length (mm) leg surface area (mm^2)	200 ±5 56.5 ±1.5 11.3-0.575; 11.3+0.59
R_{leg}: leg resistance (Ω)	142 ±50

Table 3.3: Range of values for parameters to be varied in the sensitivity analysis

By carrying out this sensitivity analysis, several features of the hydrophone sensitivity may be modified. The ones that will be examined include:

- change in sensitivity at 1 MHz
- change in sensitivity at resonance
- change in sensitivity at 30 MHz
- change in resonance frequency
- ratio of sensitivity at resonance to sensitivity at 1 MHz.

3.3.2.1 Gold, chromium and pvdf thickness

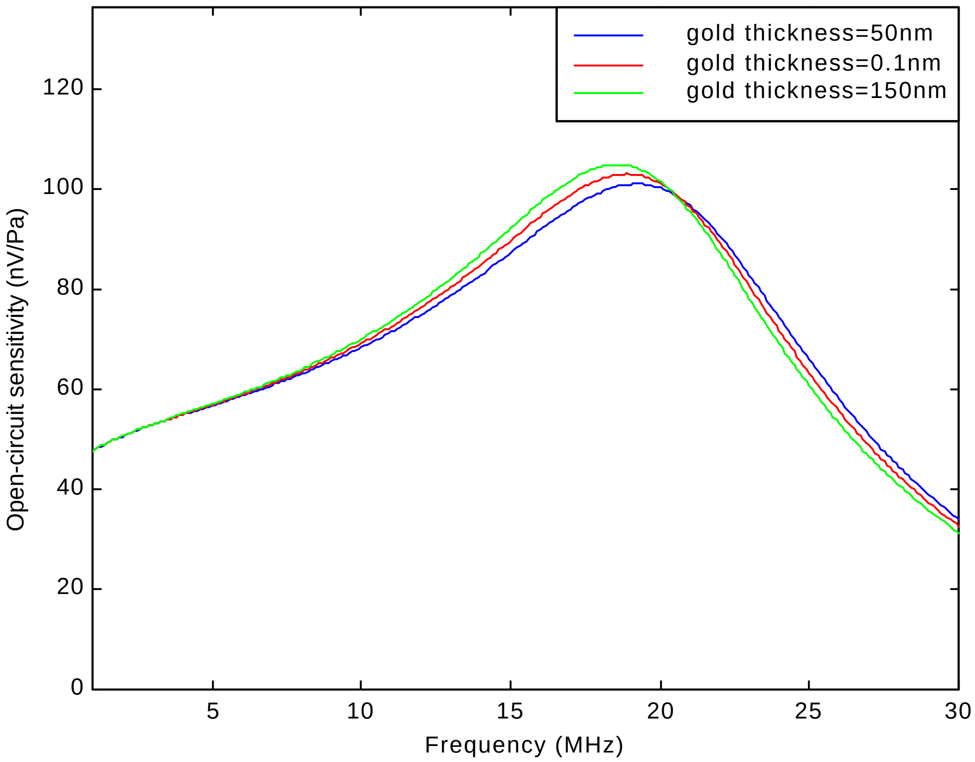

Figure 3.11: Changes in bilaminar sensitivity when the gold layer thickness is varied as described in Table 3.3.

Although the thickness of the gold layer is small relative to the thickness of pvdf, the characteristic impedance of gold is much larger than that of pvdf. Small changes in gold thickness therefore have a non-negligible effect. As the thickness of each gold layer is increased, the resonance frequency decreases and the resonance appears slightly narrower. The low-frequency sensitivity appears largely unaffected by the changes in gold layer thickness.

	Sensitivity at 1 MHz (nV Pa^{-1}); percentage change	Sensitivity at resonance (nV Pa^{-1}); percentage change	Sensitivity at 30 MHz (nV Pa^{-1}); percentage change	Resonance frequency (MHz); percentage change	Ratio of sensitivity at 1 MHz to sensitivity at resonance
gold thickness 0.1 μm	47.5	103	32.6	18.9	2.17
gold thickness 0.05 μm (-50%)	47.5	101 (-1.89%)	33.9 (+4.17%)	19.2 (+1.59%)	2.13 (-1.88%)
gold thickness 0.15μm (+50%)	47.5	105 (+1.86%)	31.3 (-3.86%)	18.6 (-1.59%)	2.21 (+1.85%)

Table 3.4: Effects of variation of gold thickness on hydrophone sensitivity.

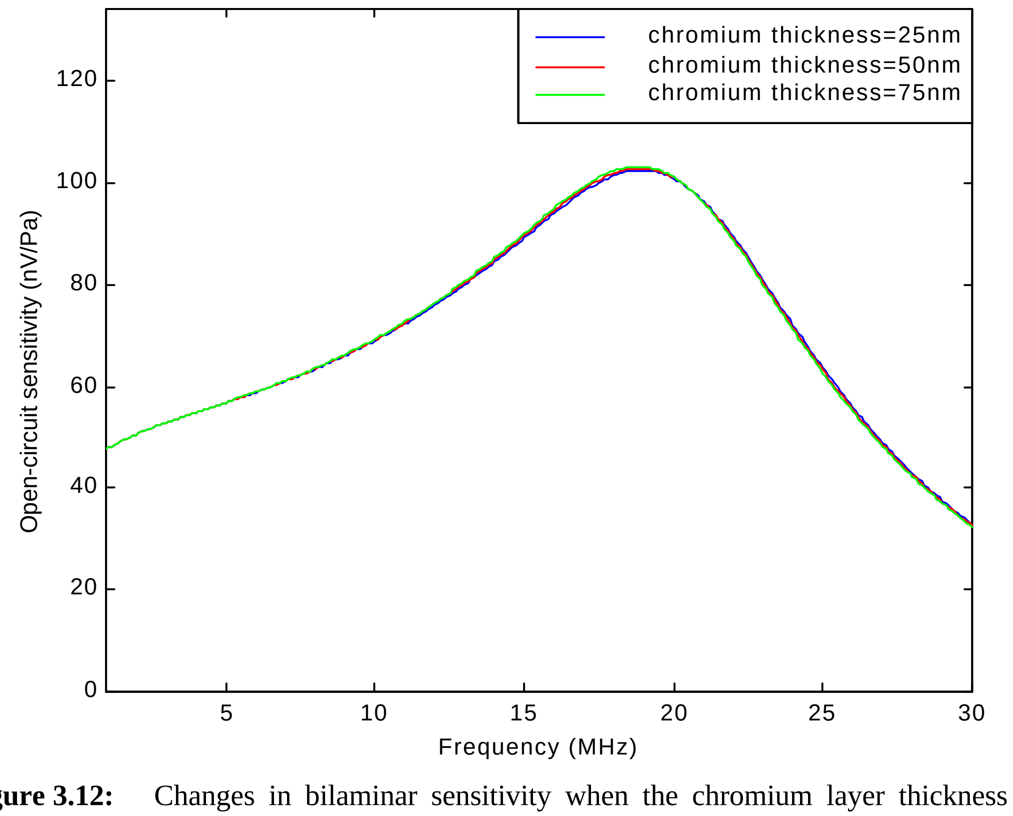

Figure 3.12: Changes in bilaminar sensitivity when the chromium layer thickness is varied as described in Table 3.3.

It can be seen that variations in the thickness of the chromium layers does not affect the overall sensitivity much compared to the previous case for the gold layers. The reasons for this are that the characteristic impedance of chromium is closer to that of pvdf than that of gold is and also that the thickness variations are relatively small.

	Sensitivity at 1 MHz (nV Pa^{-1}); percentage change	Sensitivity at resonance (nV Pa^{-1}); percentage change	Sensitivity at 30 MHz (nV Pa^{-1}); percentage change	Resonance frequency (MHz); percentage change	Ratio of sensitivity at 1 MHz to sensitivity at resonance
Chromium thickness: 50 nm	47.5	103	32.6	18.9	2.17
Chromium thickness: 25 nm (-50%)	47.5 (0%)	103 (0%)	32.8 (+0.7%)	18.9 (0%)	2.16 (-0.3%)
Chromium thickness: 75 nm (+50%)	47.5 (0%)	103 (0%)	32.3 (-0.7%)	18.8 (-0.5%)	2.18 (+0.3%)

Table 3.5: Effects of variation of pvdf thickness on hydrophone sensitivity.

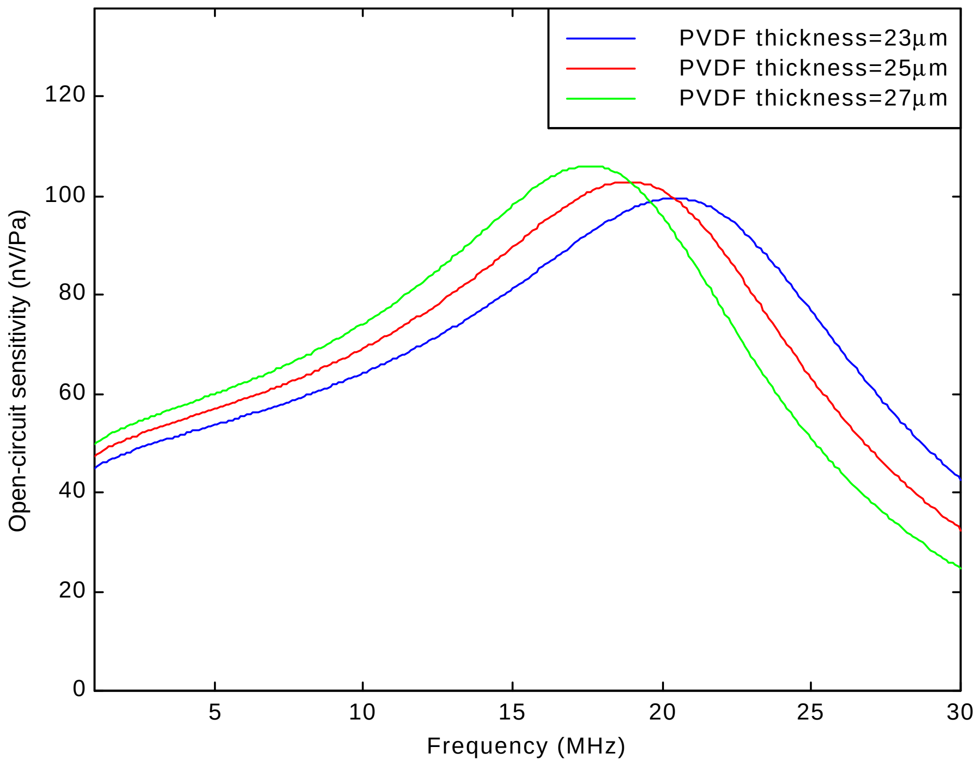

Figure 3.13: Changes in bilaminar sensitivity when the pvdf layer thickness is varied as described in Table 3.3.

Changes in pvdf thickness have a radical effect on the hydrophone sensitivity. Not only are the acoustical characteristics of the hydrophone modified, but so are the capacitances associated with the active element and with the leg. As with the gold, an increase in pvdf thickness affects the resonance frequency by shifting it toward the left and by narrowing the resonance. If the thickness of the pvdf layers is set to 25 µm, the resonance occurs at a frequency of about 18.8 MHz. Lowering this thickness by 2 µm increases the resonance to 20.4 MHz whereas increasing the pvdf thickness by 2 µm causes the resonance frequency to shift to 17.5 MHz. The low frequency sensitivity tends to increase with the pvdf thickness. This result is to be expected since, to a first order approximation, the *e.m.f* of an equivalent voltage source associated with a layer of pvdf is proportional to its thickness (18). For the input parameters in Table 3.3, at 1 MHz, a –2 µm change in pvdf thickness causes a –5.5% shift in the sensitivity whereas a +2 µm change in pvdf thickness causes a +5.2% shift in the sensitivity.

	Sensitivity at 1 MHz (nV Pa^{-1}); percentage change	Sensitivity at resonance (nV Pa^{-1}); percentage change	Sensitivity at 30 MHz (nV Pa^{-1}); percentage change	Resonance frequency (MHz); percentage change	Ratio of sensitivity at 1 MHz to sensitivity at resonance
pvdf thickness: 25 µm	47.5	103	32.6	18.9	2.17
pvdf thickness: 23 µm (-8%)	44.9 (-5.47%)	99.6 (-3.32%)	42.6 (+30.8%)	20.4 (+7.94%)	2.22 (+2.28%)
pvdf thickness: 27 µm (+8%)	49.9 (+5.16%)	106 (+3.07 %)	24.6 (-24.5%)	17.6 (-6.88%)	2.13 (-1.98%)

Table 3.6: Effects of variation of pvdf thickness on hydrophone sensitivity.

3.3.2.2 Piezoelectric coefficient d_{33}

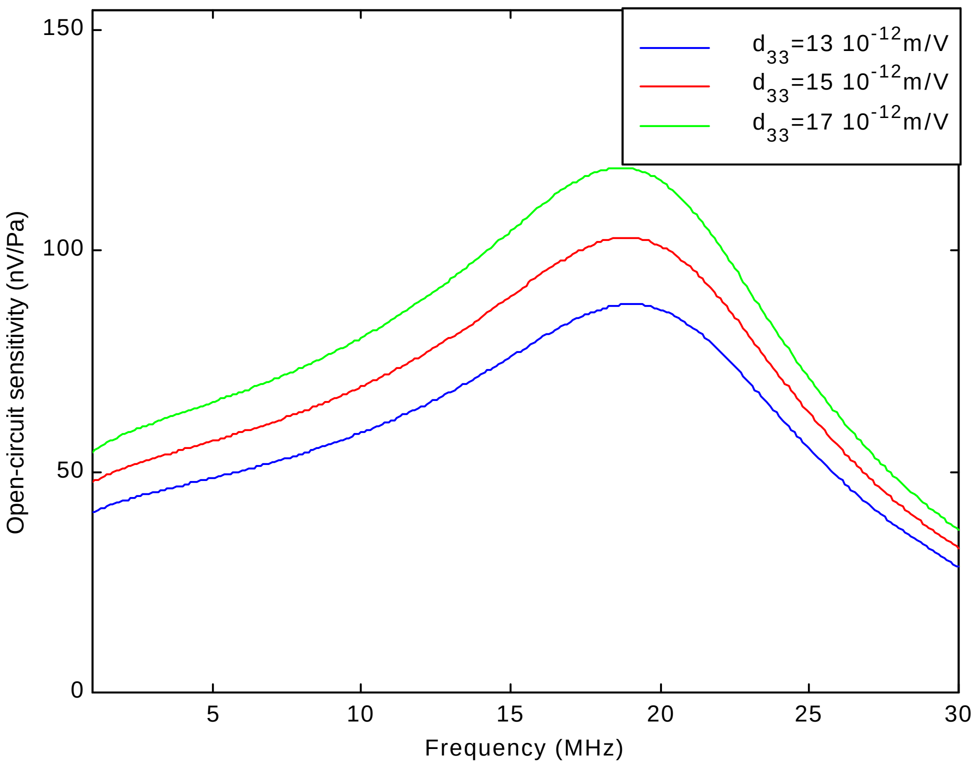

Figure 3.14: Changes in bilaminar sensitivity when the piezoelectric coefficient d_{33} is varied as described in Table 3.3.

To a first order approximation, the d_{33} piezoelectric coefficient acts as a scaling factor to the overall response. Table 3.7 shows that the response at 1 MHz, 30 MHz and at resonance is scaled by roughly the same amount when d_{33} is set at 13×10^{-12} m V^{-1} and 17×10^{-12} m V^{-1} whilst the resonance frequency shift is minimal.

	Sensitivity at 1 MHz (nV Pa^{-1}); percentage change	Sensitivity at resonance (nV Pa^{-1}); percentage change	Sensitivity at 30 MHz (nV Pa^{-1}); percentage change	Resonance frequency (MHz); percentage change	Ratio of sensitivity at 1 MHz to sensitivity at resonance
d_{33}: 15×10^{-12} m V^{-1}	47.5	103	32.6	18.9	2.17
d_{33}: 13×10^{-12} m V^{-1} (-13.3%)	40.7 (-14.4%)	87.9 (-14.7%)	28.4 (-12.9%)	19.0 (+0.05%)	2.16 (-0.3%)
d_{33}: 17×10^{-12} m V^{-1} (+13.3%)	54.6 (+14.9)	119 (+15.4%)	36.7 (+12.6%)	18.7 (-1.06%)	2.18 (+0.4%)

Table 3.7: Effects of variation of piezoelectric coefficient d_{33} on hydrophone sensitivity.

3.3.2.3 Element diameter

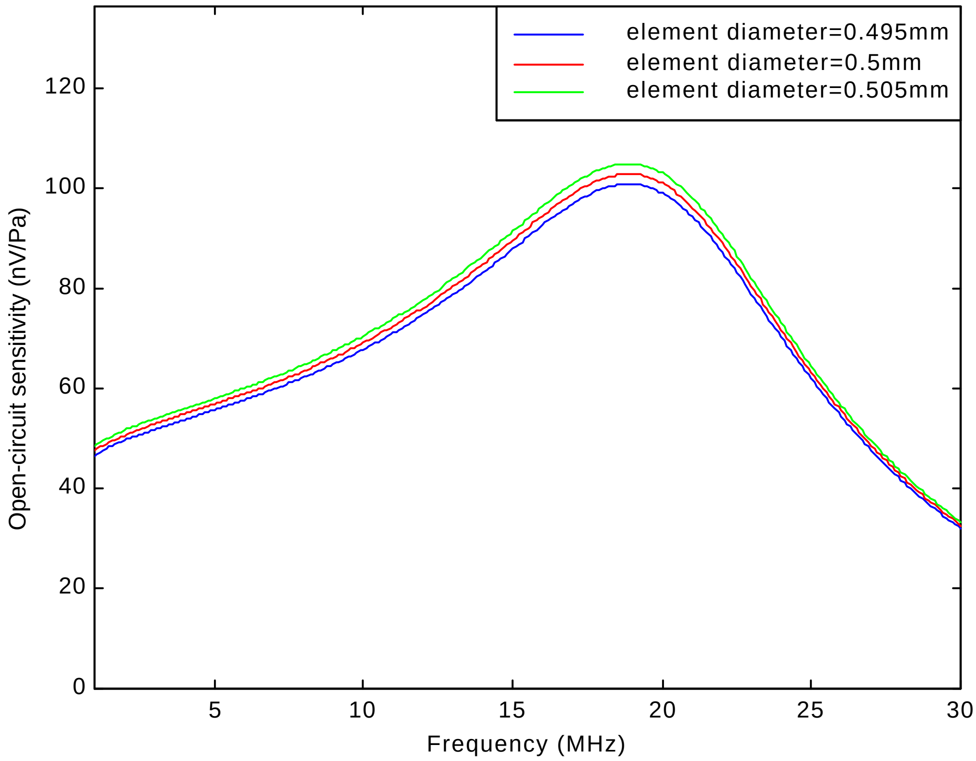

Figure 3.15: Changes in bilaminar sensitivity when the element diameter is varied as described in Table 3.3.

The overall hydrophone sensitivity appears to increase with the element diameter. The latter quantity defines the values of the element and leg capacitances.

	Sensitivity at 1 MHz (nV Pa^{-1}); percentage change	Sensitivity at resonance (nV Pa^{-1}); percentage change	Sensitivity at 30 MHz (nV Pa^{-1}); percentage change	Resonance frequency (MHz); percentage change	Ratio of sensitivity at 1 MHz to sensitivity at resonance
Element diameter: 0.5 mm	47.5	103	32.6	18.9	2.17
Element diameter: 0.495 mm (-1%)	46.5 (-1.97)	101 (-1.97%)	31.9 (-1.97%)	18.9 (0%)	2.17 (0%)
Element diameter: 0.505 mm (+1%)	48.4 (+1.99)	105 (+1.98%)	33.2 (+1.99%)	18.9 (0%)	2.17 (0%)

Table 3.8: Effects of variation of element diameter on hydrophone sensitivity.

3.3.2.4 Leg surface area

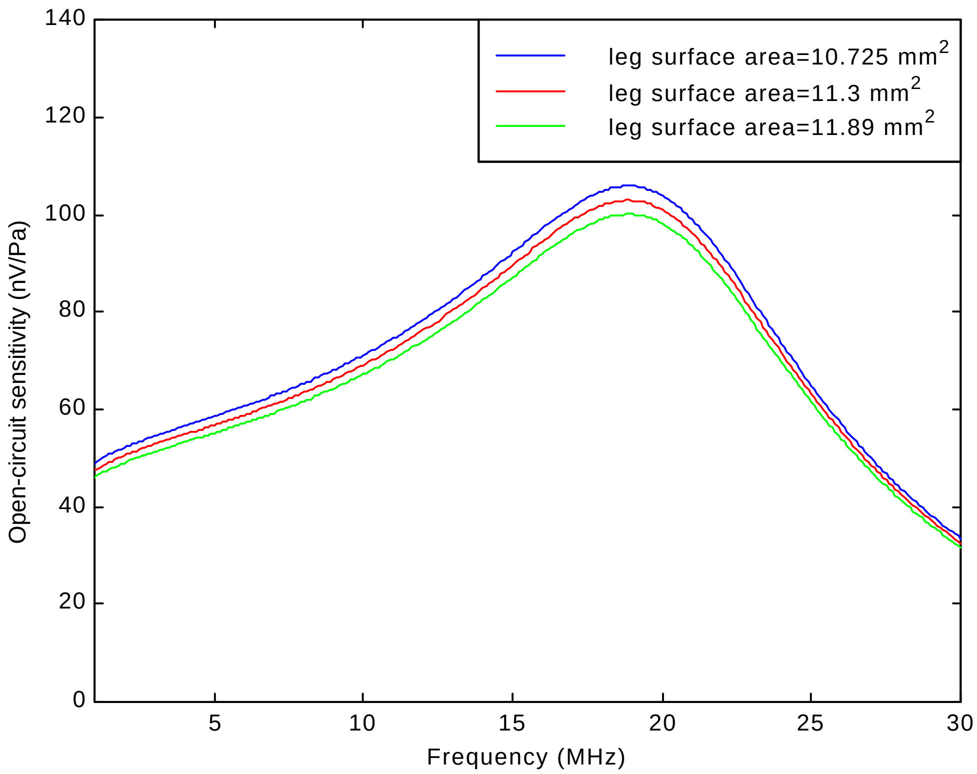

Figure 3.16: Changes in bilaminar sensitivity when the leg surface area is varied as described in Table 3.3.

Small changes in leg surface area appear to shift the response along the *y*-axis without affecting the resonance frequency. As the leg surface area increases, the response tends to drop.

	Sensitivity at 1 MHz (nV Pa^{-1}); percentage change	Sensitivity at resonance (nV Pa^{-1}); percentage change	Sensitivity at 30 MHz (nV Pa^{-1}); percentage change	Resonance frequency (MHz); percentage change	Ratio of sensitivity at 1 MHz to sensitivity at resonance
Leg surface area: 11.3 mm^2	47.5	103	32.6	18.9	2.17
Leg surface area: 10.725 mm^2 (-5.09%)	49.0 (+3.26%)	106 (+2.85%)	33.5 (2.82%)	18.9 (0%)	2.16 (-0.4%)
Leg surface area: 11.89 mm^2 (+5.22%)	46.0 (-3.14%)	100 (-2.78%)	31.7 (-2.76%)	18.9 (0%)	2.18 (+0.4%)

Table 3.9: Effects of variation of leg surface area on hydrophone sensitivity.

3.3.2.5 Leg resistance

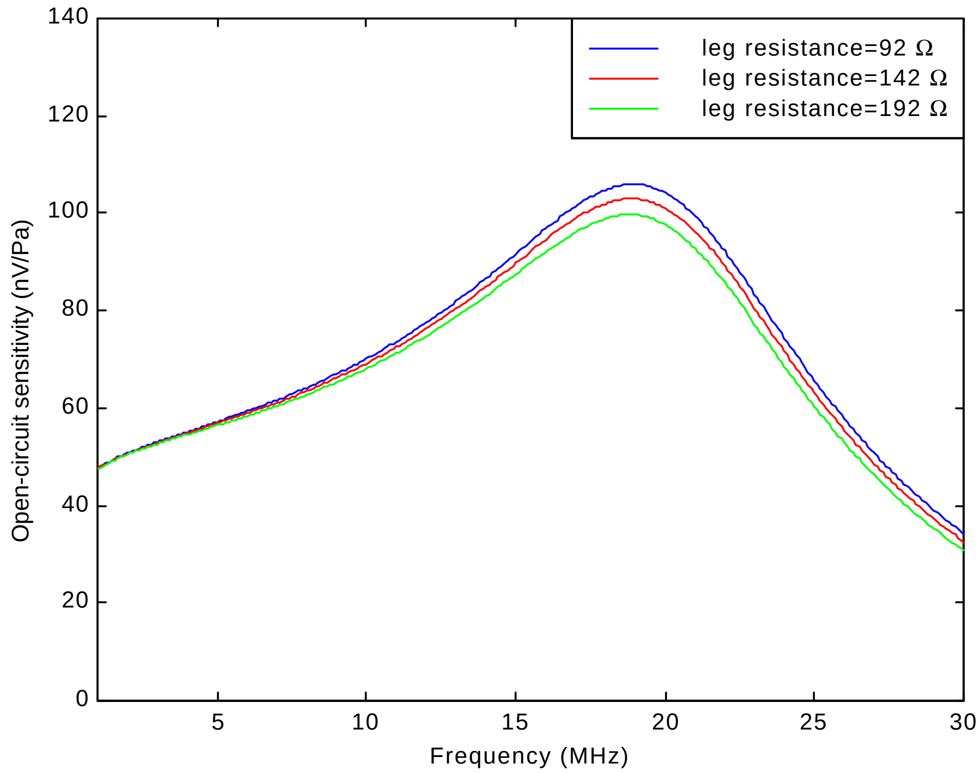

Figure 3.17: Changes in bilaminar sensitivity when the leg resistance is varied as described in Table 3.3.

Variations in the leg resistance do not appear to affect the low frequency sensitivity much. However, at frequencies approaching and beyond resonance, the sensitivity decreases as the leg resistance increases. This is expected since dissipative mechanisms tend to affect systems mostly around resonances.

	Sensitivity at 1 MHz (nV Pa^{-1}); percentage change	Sensitivity at resonance (nV Pa^{-1}); percentage change	Sensitivity at 30 MHz (nV Pa^{-1}); percentage change	Resonance frequency (MHz); percentage change	Ratio of sensitivity at 1 MHz to sensitivity at resonance
Leg resistance: 142 Ω	47.5	103	32.6	18.9	2.17
Leg resistance: 92 Ω (-35.2%)	47.5 (0%)	106 (+2.89%)	34.2 (+5.07%)	18.9 (0%)	2.23 (+2.77%)
Leg resistance: 192 Ω (+35.2%)	47.4 (-0.1%)	99.7 (-3.19%)	30.8 (-5.53%)	18.8 (-0.5%)	2.10 (-3.07%)

Table 3.10: Effects of variation of leg resistance on hydrophone sensitivity.

3.3.2.6 Relative dielectric constant

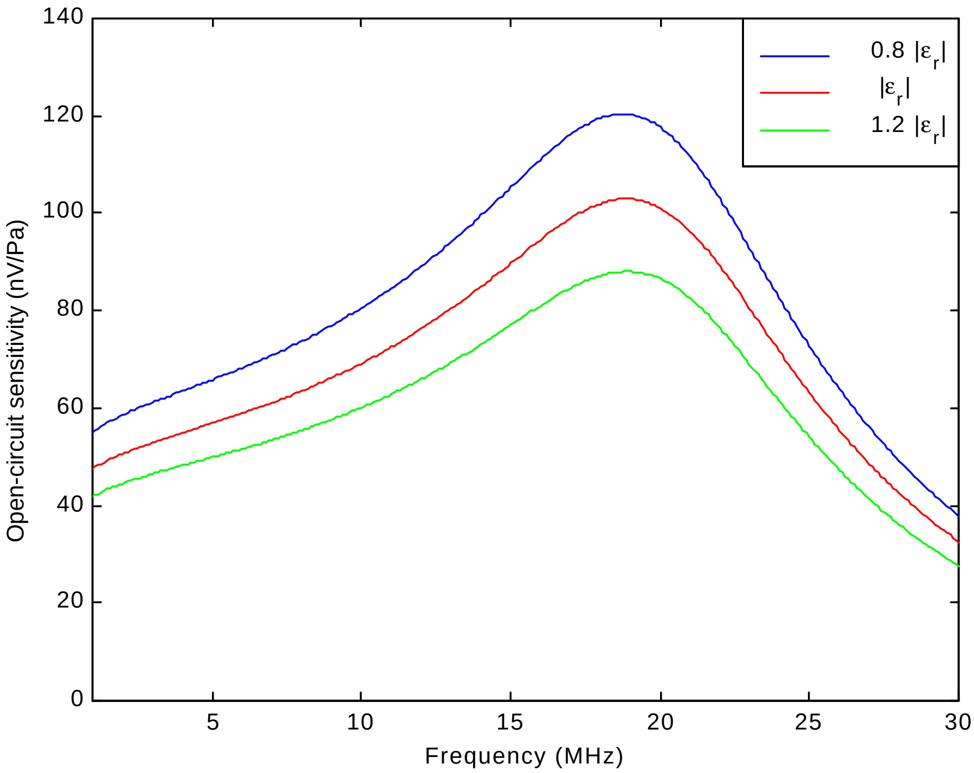

Figure 3.18: Changes in bilaminar sensitivity when the modulus of the relative permittivity is varied as described in Table 3.3.

It can be seen that the relative permittivity of pvdf has a crucial effect on the overall response. This quantity not only governs the conversion of pressure to voltage in a piezoelectric material, but will also affect the values of the element and leg capacitances. Three independent measurements of this quantity on a failed bilaminar device yielded large uncertainties as to its variation with frequency: a mean value of around 10 ± 4 at 1 MHz. The variations imposed here are therefore by no means unreasonable and these cause comparatively large changes in the overall response. Generally, the sensitivity will decrease as the relative permittivity increases. If there are large variations in this parameter from one hydrophone to another, it is clear that a range of corresponding sensitivities is to be expected.

	Sensitivity at 1 MHz (nV Pa^{-1}); percentage change	Sensitivity at resonance (nV Pa^{-1}); percentage change	Sensitivity at 30 MHz (nV Pa^{-1}); percentage change	Resonance frequency (MHz); percentage change	Ratio of sensitivity at 1 MHz to sensitivity at resonance
$\|e_r\|$	47.5	103	32.6	18.9	2.17
0.8$\|e_r\|$ (-20%)	55.1 (16.0%)	120 (+16.9%)	37.8 (16.1%)	18.7 (-1%)	2.18 (+0.8%)
1.2$\|e_r\|$ (+20%)	41.7 (-12.1%)	88.1 (-14.4%)	27.4 (-15.7%)	18.9 (0%)	2.11 (-2.72%)

Table 3.11: Effects of variation of modulus of relative permittivity of pvdf on hydrophone sensitivity.

3.4 DEVELOPMENT TOOLS

3.4.1 Establishment of a User Specification based on the output of Phase 1

This section describes an implementation of the model using the mathematical software package MATLAB.

From analysis of the user survey, it has been noted that various shielded bilaminar hydrophones are used over a range of frequencies. The user therefore needs to be given the option to specify the frequency range of interest, as well as the parameters which will characterise the hydrophone, i.e. the pvdf film thickness and the element diameter.

Cables of various lengths may be used, so this parameter also features in the list of data to be entered by the user.

The survey revealed that the hydrophones are generally used under three types of conditions:

- open circuit
- with an oscilloscope
- with an amplifier followed by a load.

It is therefore desirable to cater for all three conditions as well as the case of an arbitrary load across the cable termination.

In the case where the hydrophone cable is connected directly to an oscilloscope, the load impedance seen at the cable termination is equivalent to a parallel combination of a DC resistance and a capacitance. The user is given the option to enter these values.

In the case where an amplifier is connected to the cable termination, the latter effectively sees the combined effect of the amplifier input impedance with the impedance of the load connected to the output terminals of the amplifier. If the device draws minimal current, the effects of the loading may be ignored when making the input impedance measurement, but this is left up to the user. Since various types of amplifiers and amplifier loads appeared in the user survey, it is best to let the user measure the loaded amplifier input impedance and complex gain as a function of frequency and store these quantities in external files that may be recalled by the program.

Additional options include allowing the user to enter different values for the thickness of each pvdf film and also to specify a depoled region in the pvdf. The user is also free to create his/her own material properties file in which the material density, sound speed, attenuation coefficient and thickness can be specified for any combination of layers and semi-infinite media on either side of the hydrophone. For example, the user may want to investigate the changes in hydrophone sensitivity caused by varying the characteristic impedance of water (and hence the water temperature). In this case, the user is no longer prompted for the pvdf thickness. The data must be entered as a matrix in an external file with a *dat* extension. This matrix must have four rows respectively corresponding to:

- material density (kg m^{-3})
- sound speed (m s^{-1})
- attenuation (N m^{-1} MHz^{-1})
- layer thickness (m)

The first column refers to the properties of the medium backing the hydrophone, the second column to those of the layer of the hydrophone that is the closest to the backing medium etc. The penultimate column refers to the properties of the front layer of the hydrophone and the last to those of the medium at the front of the hydrophone. As the media on either side of the hydrophone are semi-infinite, there is no thickness associated with these and *inf* may be used in the file, although any number will do as these will not used in the main program. An example of a file is shown below:

998.2	19281	7194	1780	1780	7194	19281	1000	1780	1780	7194	19281	998.2
1482.36	3240	6609	2300	2300	6609	3240	1600	2300	2300	6609	3240	1482.36
0	0	0	111	111	0	0	105	111	111	0	0	0
inf	1E-7	50E-9	0.7E-6	24.3E-6	50E-9	1E-7	0.5E-6	0.7E-6	24.3E-6	50E-9	1E-7	inf

Summary of input data to be entered by the user:

- material properties file to be used: default or user-defined
- range of frequencies for analysis
- pvdf thickness of each layer
- thickness of depoled region in each pvdf layer
- element diameter
- cable length
- type of load impedance:

    a. open circuit cable: load impedance $Z_L \rightarrow \infty$
    b. parallel combination of resistance and capacitance, values of which to be specified by the user
    c. user-defined: load data is extracted from a user-defined file containing the real and imaginary parts of the load impedance as a function of frequency
    d. loaded amplifier: input impedance and complex gain data are extracted from two user-defined files containing their real and imaginary parts as a function of frequency.

Note that all input and output files are to have a *dat* extension

3.4.2 Description and validation of MATLAB code in compliance with NPL Quality procedure (for Level 3 software)

3.4.2.1 Description of MATLAB code

The code essentially follows the theory outlined in Section 3.2.2 and incorporates a user interface, the basis for which is described in Section 3.4.1. The main steps of the program will be briefly described here. The reader is referred to Section 3.2.2 for more information.

The user is first asked whether he/she wishes to use the default material properties file or a user defined one. These files will contain the density, sound speed, attenuation and thickness of each layer of material in the hydrophone and of the semi-infinite media on either side. The characteristic impedance is then computed for each layer.

The user is then asked to enter the range of frequencies over which the hydrophone sensitivity is to be calculated. This allows the computation of the wave number as a function of frequency for each material.

The element properties are then evaluated. The user is prompted for the element diameter, for the thickness of each pvdf layer and for the depoled region thickness. The last two properties are not required if the user specifies a user-defined file for the material properties. The impedances associated with the lossy element capacitances are then calculated.

The transfer characteristics of the leg are computed, followed by those of the cable, after the user has entered a value for the cable length.

The user is then given a list of loads to chose from, as described in Section 3.4.1. Amplifier data is to be supplied via an external file. The electrical impedance of the equivalent electrical network connected to the element is then computed.

In Section 3.2.2.2.B, it was seen that an iterative procedure needs to be adopted in order to compute the *e.m.f.*'s of the equivalent voltage sources in Figure 3.4. The components of the transfer matrices of each layer are computed as a function of frequency and piezoelectric effects are first ignored. By means of the transfer matrix method described in Section 3.2.2.1, the particle velocities at each extremity of the layers of pvdf may be computed and a first approximation for the *e.m.f.*'s of the equivalent voltage sources are then obtained. From the second iteration onwards, the piezoelectric terms are included in the transfer matrices for the pvdf layers. The iteration is repeated until convergence of the *e.m.f.* values. For convergence up to at least six significant figures, seven iterations are usually necessary.

By knowledge of the voltage supplied by the two equivalent voltage sources in Figure 3.4, the voltage across the load at the cable termination may be obtained through use of the transfer matrices of the leg and cable. In the case where the cable termination is connected to a loaded amplifier the output voltage is evaluated from knowledge of the gain and input impedance of the complete amplifier-load system.

The transfer characteristics are finally plotted in phase and magnitude and the user is then asked whether he/she wants the results to be stored in a data file. All output files automatically have a *dat* extension associated with them.

3.4.2.2 Validation of MATLAB code

A Pressure to pvdf voltage transfer

In order to validate the code, some extreme cases will be considered. A crude model of a coplanar hydrophone where secondary piezoelectric effects are accounted for is presented in (17). From a geometrical point of view, in the current model, if the thickness of all structural layers are made very small except for that of one pvdf layer, the model will then tend to that described in (17). The electrical impedance associated with the element capacitance of the very thin pvdf layer must be made very large, if the electrical equivalent circuits of both models are to match. The expression for the sensitivity in (17) does not account for leg and cable effects or for the presence of gold layers: it simply computes the output voltage across a load impedance Z_E for a unit pressure wave incident on the pvdf. Hence, arbitrary values for Z_E will be chosen and the voltages across these loads compared for a unit incident pressure wave.

The input parameters are presented in Table 3.12.

r: material density (kg m^{-3})	water: 998.2; gold: 19281; chromium: 7194; pvdf: 1780; glue: 1000
c: velocity of sound (m s^{-1})	water: 1500; gold: 3240; chromium: 6608; pvdf: 2300; glue 1600
L: thickness of layer (μm)	gold: 10^{-10}; chromium: 10^{-10}; rear pvdf (poled+depoled): 25; front pvdf 10^{-10}; depoled front pvdf region: 10^{-10}; glue: 10^{-10}
a: attenuation coefficient (neper m^{-1} MHz^{-1})	pvdf: 111; glue: 104
d_{33}: piezoelectric coefficient (pC N^{-1})	15
e_0: dielectric constant (pF m^{-1})	8.85
$\|e_r\|$: modulus of relative permittivity of pvdf (as a function of frequency f in Hz)	$-2.82 \log_{10}(f)+26.7$
tan d: loss tangent of relative permittivity of pvdf (as a function of frequency f in MHz)	$0.22 + 0.07 \log_{10}(f) - 0.055 \log_{10}(f)^2$
r: element radius (mm)	0.25
Z_E: electrical impedance (Ω)	100, 10^{60}
$Z_{el,2}$: impedance of lossy capacitance of front pvdf (Ω)	10^{60}

Table 3.12: Input parameters for model verification.

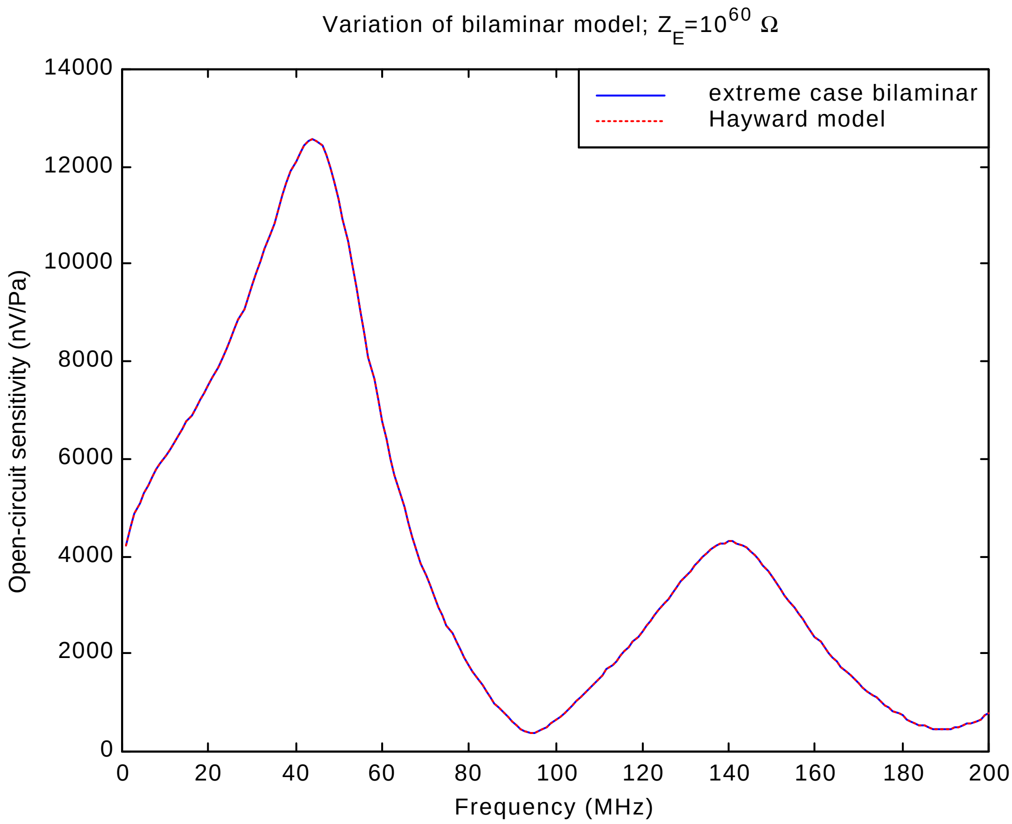

Figure 3.19: Sensitivity comparison between the extreme case bilaminar and the model in (17) for a 10^{60} load resistor connected to the element (approximates open circuit conditions).

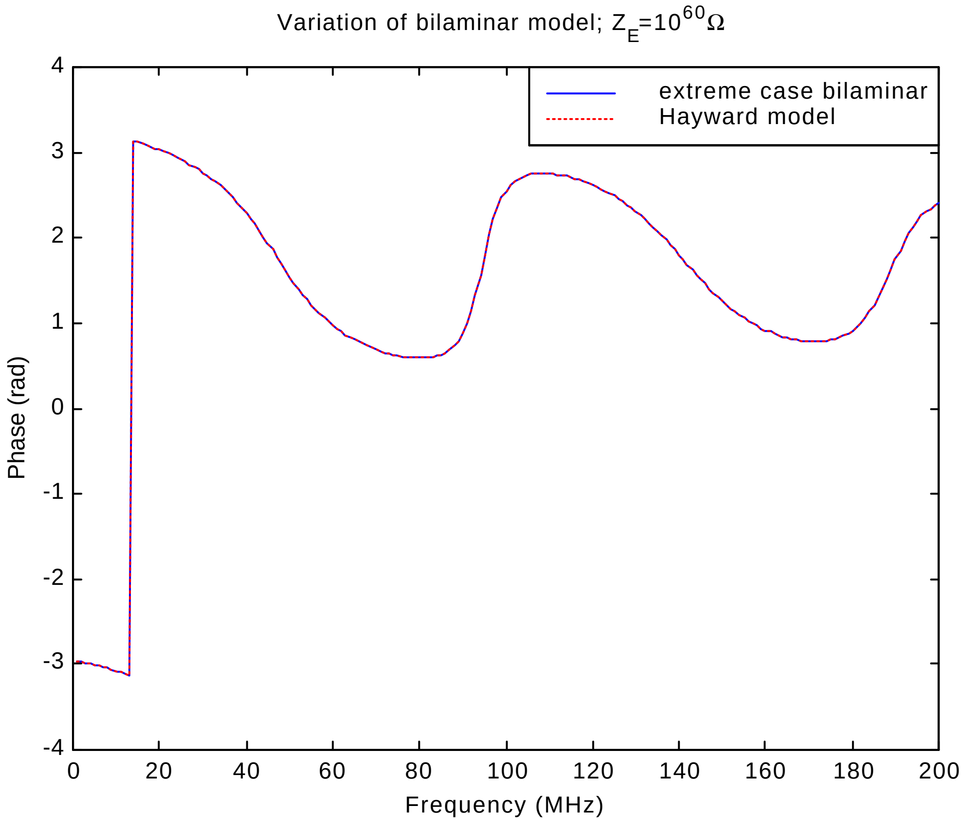

Figure 3.20: Phase comparison between the extreme case bilaminar and the model in (17) for a 10^{60} load resistor connected to the element (approximates open circuit conditions).

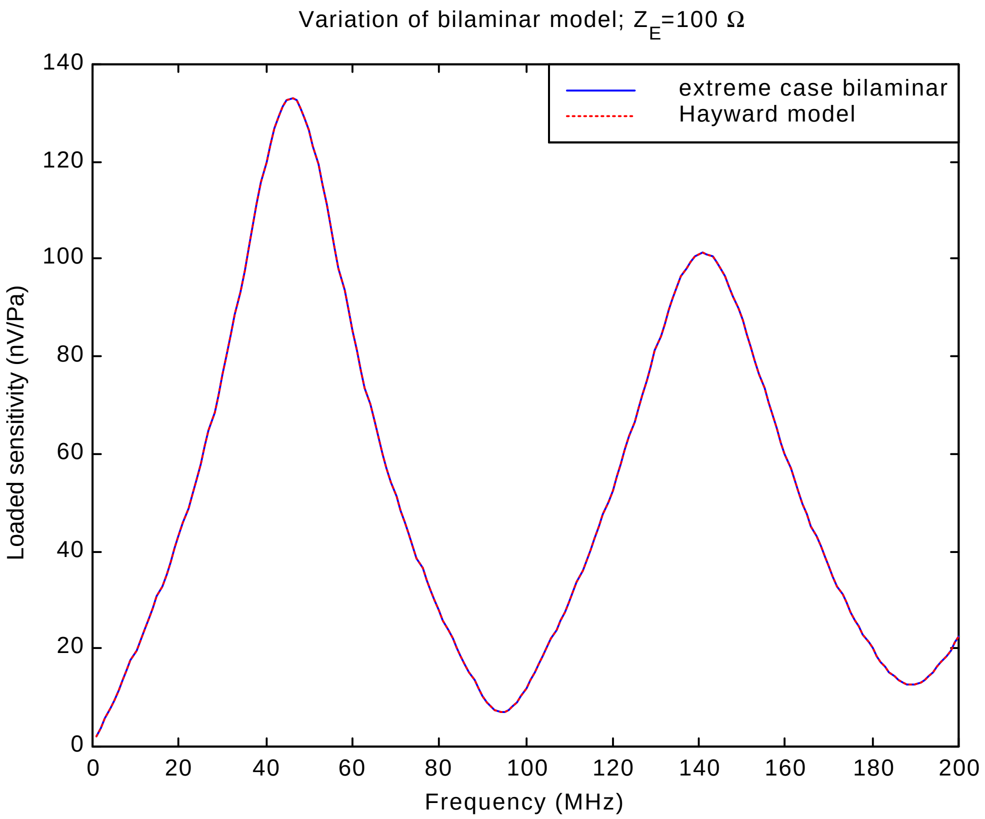

Figure 21: Sensitivity comparison between the extreme case bilaminar and the model in (17) for a 100 Ω load resistor connected to the element.

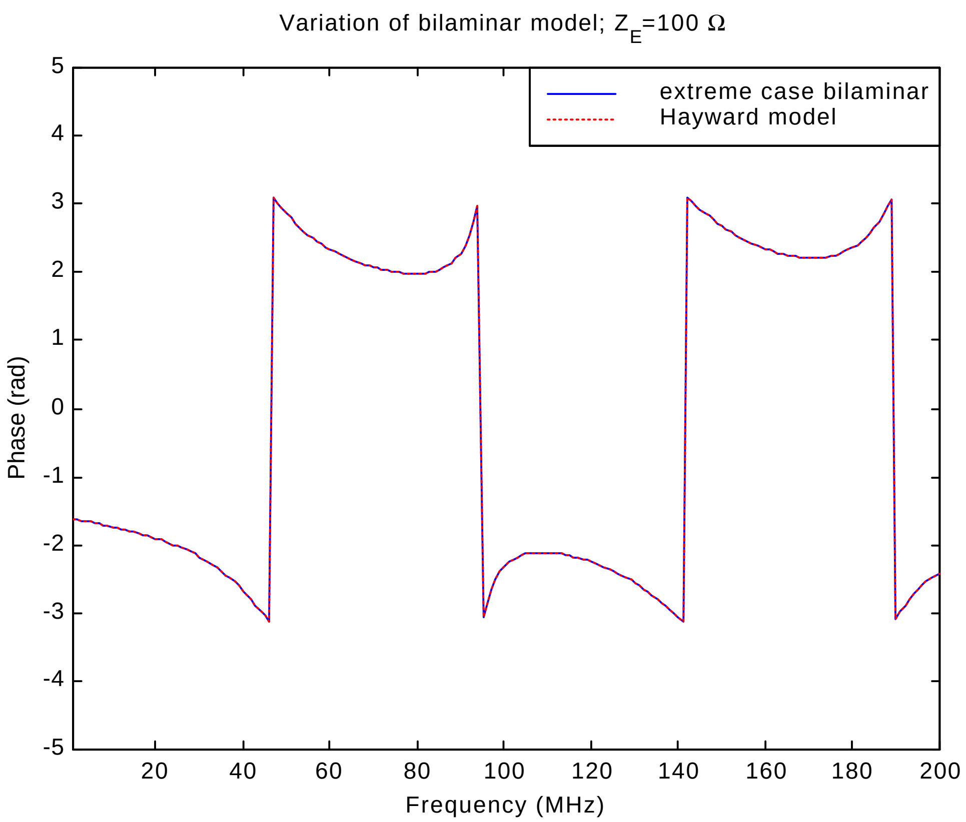

Figure 22: Phase comparison between the extreme case bilaminar and the model in (17) for a 100 Ω load resistor connected to the element.

Figures 3.19 to 3.22 show that there are no visible differences between the two models under the above-described conditions.

B Leg transfer

The leg network code may be validated for extreme values of the series resistances. If the overall leg resistance tends to zero, the input impedance of the leg with an open circuit termination will tend to that of the leg capacitance.

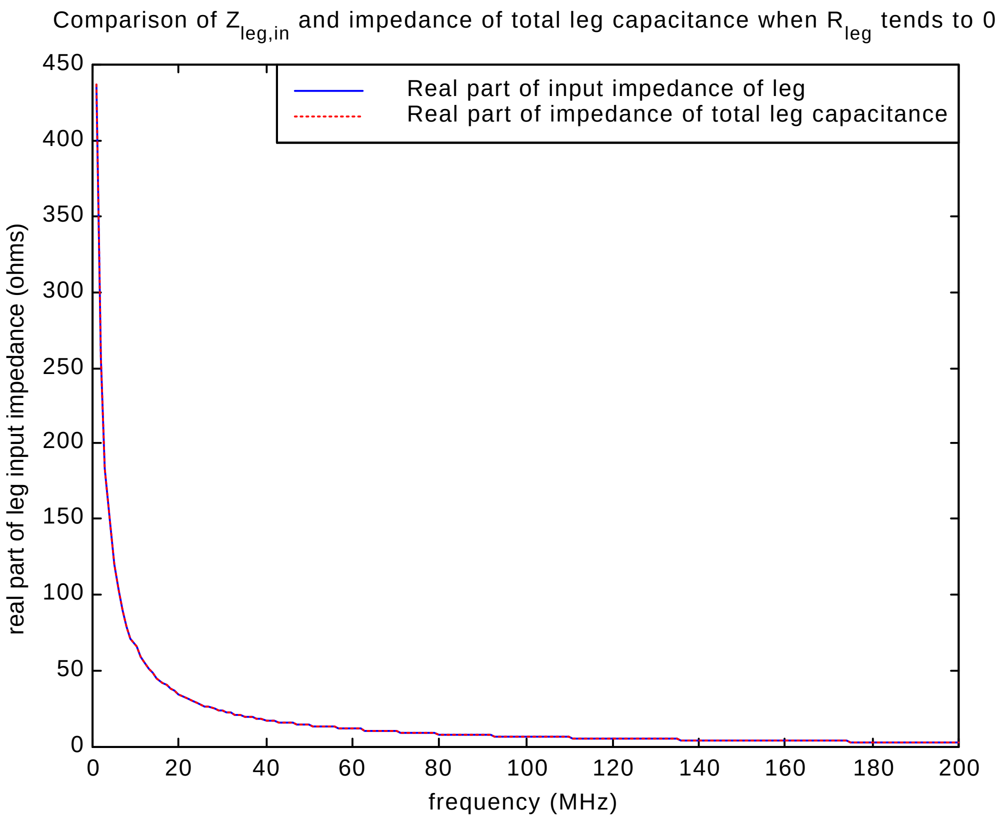

Figure 3.23: Comparison between real parts of leg impedance and impedance of total leg lossy capacitance when the total leg resistance tends to zero. The leg termination is open circuit.

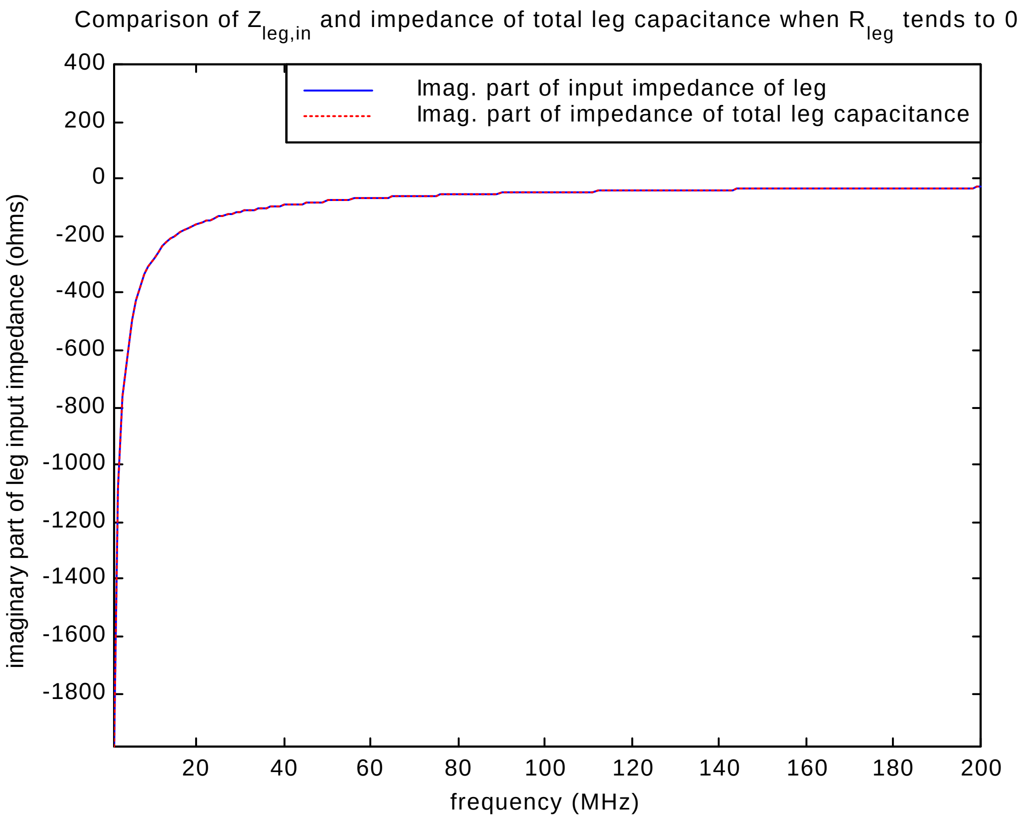

Figure 3.24: Comparison between imaginary parts of leg impedance and impedance of total leg lossy capacitance when the total leg resistance tends to zero. The leg termination is open circuit.

There are no visible differences in the predicted leg input impedance when the leg resistance tends to zero and with the value of the total lossy leg capacitance.

4. DISCUSSION

The two main issues that arise in attempting to assess the work on the hydrophone model are:

- the accuracy of the model
- the accuracy of the model input parameters.

Without a good knowledge of the latter, it is difficult to objectively assess the former. What has been done in Section 3.3.2 however shows that, if the model input parameters are varied within plausible ranges, the obtained hydrophone response generally appears to be within the limits expected from calibration results (see Section 3.3.1). However, it is not possible to say at this stage whether, if a bilaminar hydrophone having the characteristics shown in Table 3.2 were to be constructed, it would produce a response approaching the one predicted by the model.

Assuming some degree of accuracy in the model, the sensitivity analysis has shown that the largest source of error in this analysis is likely to come from inadequate characterisation of the following input parameters:

- the pvdf film thickness
- the value of the piezoelectric coefficient d_{33}
- the value of the relative permittivity of pvdf e_r.

The pvdf film thickness will tend to affect the position of the resonance, as seen in Section 3.3.2.1. It is debatable as to whether or not a depoled region should be included in the pvdf. Again, this would be something to examine once the model input parameters are more accurately known, as this would allow the effects associated with this depoled region to be isolated from effects due to, say, variations in the thickness of the gold layers on a given device.

It should be noted that there is a degree of uncertainty as to the material properties of pvdf itself. Due to the various types of commercially available pvdf, getting accurate data for the characteristic impedance can prove to be difficult.

In this work, the value of d_{33} has been assumed to be constant with frequency. A measurement of this quantity with frequency would not be straightforward, but would nevertheless provide more confidence in the model. However, judging by the comparatively large effect that small variations in this quantity has on the predicted response, and the good agreement with calibration results, it is likely that d_{33} does not vary much in the 1-30 MHz frequency range.

It was shown that the random and systematic errors in the measurement of $|e_r|$ cause the corresponding hydrophone sensitivities to span a large range (see Section 3.3.2.6). From the sensitivity analysis, it would appear that this quantity is potentially the largest source of error. Better characterisation of both the magnitude and phase (and hence the loss tangent) of this quantity appear essential. This may unfortunately not be so straightforward, as three independent measurements of $|e_r|$ on the same membrane have yielded different results (see Figure 3.18). Also, the values obtained for $|e_r|$ beyond approximately 20 MHz may be subject to some uncertainty (see Figures 3.8 and 3.9). It is possible that the increase in $|e_r|$ is due to an inductive component which starts to dominate the response, but this could also be a problem associated with the measurement.

Regarding the accuracy of the model, it should be noted that piezoelectric effects due to d_{31} have not been taken into account. Each pvdf layer has been assumed to be infinite in the y and z directions, x being the direction of propagation. Strictly speaking, even in the case of a plane-wave incident on the hydrophone, some Poisson's ratio effects will occur and piezoelectric effects due to the d_{31} coefficient may affect the overall response.

Also, it is unlikely that the thickness of each layer will be the same throughout the surface area of the device. Accounting for this is however beyond the capabilities of the one-dimensional model presented here and would require a three-dimensional model to be developed. In this case, identifiable trends would have to be observed in the configuration of the layers of materials from one device to another.

A two-port network characterisation of the leg would have been useful in order to fully validate the theoretical approach.

5. SUMMARY AND CONCLUSIONS

A complete theoretical model for the transfer characteristics of a 25 µm film thickness 0.5 mm diameter bilaminar hydrophone has been developed and validated as part of project 4.4.3 of the DTI National Measurement System Programme for Acoustical Metrology, 1998-2001.

The model includes:

- the possibility to model one-dimensional acoustic propagation in multi-layered media using a transfer matrix formulation
- secondary piezoelectric effects
- the electrical effects of the leg, modelled as a distributed series resistance/shunt lossy capacitance network
- the hydrophone coaxial cable, modelled as a transmission line, followed by a load if required
- the amplifier transfer characteristics, the properties of which are to be obtained from measurement.

Precision Acoustics Ltd has contributed to this project by producing measurements of some of the model input parameters.

The open-circuit response predicted by the model compares well with calibration results and varying the model input parameters within plausible ranges appears to reproduce the trends observed in the responses of calibrated devices.

The validation process was not as complete as it would have been had the work in the original project proposal been carried out. In particular, this would have included a better characterisation of the model input parameters, as well as the construction and calibration of a reference hydrophone (originally to be done by Marconi Technology Centre). As the properties of this reference device would have been better known, a more rigorous assessment of the model would have been possible.

Nevertheless, key input parameters that play an important role in the predicted response have been identified by means of a sensitivity analysis. These include:

- the relative permittivity of pvdf
- the piezoelectric coefficient of pvdf
- the film thicknesses of pvdf.

6. RECOMMENDATIONS

In the near future, there may be scope to pursue the work outlined in the original project proposal as it is planned that NPL will be assisting PA in the development of their next generation of membrane hydrophones. It is hoped that if this collaboration takes place, further light will be shed on better characterising the model parameters and on the accuracy of the model.

A best-fit routine may then be developed in which some calibration points are loaded into a program that will then vary the unknown input parameters within specific ranges so that the predicted response best fits the calibration data in a least-squares sense.

If this work is carried out and it is felt that a one-dimensional model is not comprehensive enough to fully characterise a bilaminar hydrophone, a finite element modelling approach may have to be resorted to. Processes resulting from Poisson’s ratio effects may then be accounted for, as well as possible variations in thickness across a given layer. The response to a non-plane-wave front may also be determined.

REFERENCES

[1] Food and Drug Administration, *Guide for measuring and reporting acoustic output of diagnostic ultrasound medical devices*. FDA 510(k), US FDA, Rockville, Maryland 20857, USA, 1985.

[2] IEC 61157, *Requirements for the declaration of the acoustic output of medical diagnostic ultrasonic equipment*, International Electrotechnical Commission, Geneva, Switzerland, 1992.

[3] IEC 61102, *Measurement and characterisation of ultrasonic fields using hydrophones in the frequency range 0,5 MHz to 15 MHz*, International Electrotechnical Commission, Geneva, Switzerland, 1991.

[4] IEC 61266, *Ultrasonics - Hand-held probe Doppler foetal heartbeat detectors - Performance requirements and methods of measurement and reporting*, International Electrotechnical Commission, Geneva, Switzerland, 1987.

[5] *Council Directive Concerning Medical Devices*, Official Journal of the European Communities, L169, Council Directive 93/42/EEC, June 1993.

[6] D. R. Bacon, *Characteristics of a pvdf membrane hydrophone for use in the range 1-100 MHz*. IEEE Transactions on Sonics and Ultrasonics, Vol SU-29(1), pp18-25, 1982.

[7] R. A. Smith, *The evaluation of small area membrane hydrophones*. NPL Report RSA(EXT)2, National Physical Laboratory, UK, 1989.

[8] T. J. Esward and S. P. Robinson, *Extending the frequency range of the NPL primary standard laser interferometer for hydrophone calibrations to 60 MHz*, IEEE Transactions in Ferroelectrics and Frequency Control, Vol. 46, No. 3, 737-744, (1999).

[9] R. A. Smith, *The importance of the frequency response of a hydrophone when characterising medical ultrasonic fields*. Proc. Inst. Acoustics, Vol. 8, Part 2, pp119-128, 1986.

[10] T. J . Esward, *An assessment of medical ultrasonic field measurement methods: final technical report for EC contract no. MATI-CT940064*, NPL Report CMAM 17, July 1998.

[11] IEC 61220, *Ultrasonics - fields- Guidance for the measurement and characterisation of ultrasonic fields generated by medical ultrasonic equipment using hydrophones in the frequency range 0.5 MHz to 15 MHz*, International Electrotechnical Commission, Geneva, Switzerland, 1993.

[12] *Physical Acoustics*, Vol. 1, edited by W.P. Mason (Academic, New York, 1964), Part A.

[13] *Acoustics*, L.L Beranek, (American Institute of Physics, Inc., New York 1986), p51.

[14] *Electrical Transducers and Wave filters*, W.P. Mason, (Van Nostrand, Princeton, NJ, 1948).

[15] R.W. Martin and R.A. Sigelmann, " Force and Electrical Thévenin Equivalent Electrical Circuits and Simulations for Thickness Mode Piezoelectric Transducers," J. Acoust. Soc. Am. **58**, 475-489 (1975).

[16] M. Redwood, "Transient Performance of a Piezoelectric Transducer," J. Acoust. Soc. Am. **33**, 527-536 (1961).

[17] G. Hayward, C.J. MacLeod and T.S. Durrani, "Systems Model of the Thickness Mode Piezoelectric Transducer," J. Acoust. Soc. Am. **76**(2), 369-381 (1984).

[18] C. Koch and W. Molkenstruck, "Primary Calibration of Hydrophones with Extended Frequency Range 1 to 70 MHz Using Optical Interferometry," IEEE Transactions on Ultrasonics, Ferroelectrics and Frequency Control, Vol. 46, No.5, 1303-1313, (1999).

[19] J.-L. Dion, E. Cornieles, F. Galindo and K. Agbossou, "Exact One-Dimensional Computation of Ultrasonic Transducers with Several Piezoelectric Elements and Passive Layers using the Transmission Line Analogy," IEEE Transactions on Ultrasonics, Ferroelectrics and Frequency Control, Vol. 44, No.5, 1120-1131, (1997).

[20] B. Rashidian and M. Rahnavard, "A Translational Matrix Formulation for an Arbitrarily Interconnected Stack of Piezoelectric Transducers," IEEE Transactions on Ultrasonics, Ferroelectrics and Frequency Control, Vol. 47, No.3, 756-758, (2000).

[21] H. Ohigashi, "Electromechanical properties of polarized polyvinylidene fluoride films as studied by the piezoelectric resonance method," *J. Appl. Phys.*, vol. 47, 949-955, 1976.

[22] R.C. Preston, S.P. Robinson, B. Zeqiri. T.J. Esward, P.N. Gelat and N.D. Lee, "Primary calibration of membranes hydrophones in the frequency range 0.5 MHz to 60 MHz", *Metrologia*, 1999, **36**, 331-343

[23] B. Fay, P.A. Lewin, G. Ludwig, G. M. Sessler and G. Young, " The influence of special polarization distribution on spot poled PVDF membrane hydrophone performance," *Ultrason. Med. Biol.*, **18**, 625-635, 1992.

[24] *Tables of Physical and Chemical Constants*, G. W. C. Kaye and T. H. Laby, Sixteenth Edition, (Longman, Essex, UK, 1995), p 99.

[25] *ibid* p 101.

[26] *Tables of Physical and Chemical Constants*, G. W. C. Kaye and T. H. Laby, Sixteenth Edition, (Longman, Essex, UK, 1995), p 102.

[27] *ibid* p 41.

[28] *ibid* p 213.

ANNEX A: HYDROPHONE USER SURVEY

New membrane hydrophone modelling project

The last twenty years has seen enormous growth in medical ultrasonic imaging at megahertz frequencies. Hydrophones are used to measure and characterise medical ultrasonic fields, to ensure compliance with specification standards and regulatory requirements. In 1999, the National Physical Laboratory (NPL), UK, in collaboration with industry, was commissioned by the Department of Trade and Industry (DTI) to develop, validate and publish a complete theoretical model for membrane hydrophone/amplifier transfer characteristics. The ultimate aim of this project is to enable users of these hydrophones to improve the accuracy of their measurements in the field of medical ultrasound. One of the objectives of the first phase of this project is to gather information from learned experts and the technical literature relating to the modelling of hydrophones.

We have now embarked on the information-gathering phase, so we are contacting a number of recognised experts in the area of medical ultrasonics and requesting their views on the use and modelling of hydrophones. To this end, we would like to invite you to contribute to this process by spending a few minutes answering the questions below. We would appreciate a reply as soon as possible.

1. Please describe in a few words your interests in hydrophone measurements.

2. Please describe the type of medical ultrasonic fields being measured (diagnostic, therapeutic, lithotripters etc.).

3. What accuracies do you require for different acoustical quantities (*p*+, *p*-, integral of *p* squared) ? Do you use a correction factor to account for limited hydrophone bandwidth ? If so, is it based on a published correction method such as IEC 61220 ?

4. Please describe your available hydrophone/amplifier measuring systems. Do you have any knowledge of the magnitude and phase characteristics of the amplifiers that you use ?

5. Do you currently use any hydrophone modelling techniques ? If so, which method do they rely on (please provide a reference if available) ?

6. Do you feel that a complete hydrohone/amplifier model would be of use to you ?

Your details:

Name:

Organisation:

Address:

ANNEX B: OUTCOME OF HYDROPHONE USER SURVEY

UK contacts

UK contact 1	1. Measurements of non-linear and high amplitude propagation effects in ultrasonic fields; measurements of fields to confirm numerical models of ultrasonic transducers; measurements of ultrasonic propagation through bone. 2. Diagnostic and therapeutic. 3. Ideally better than 5%. 4. Corrections based on hydrophone calibration and input impedance of measurement system. When necessary, extend beyond calibration range using simple hydrophone models. 5. Avoid amplifier. 6. Use simple extrapolation techniques to extend beyond calibration range. 7. Yes, especially for phase data for accurate estimate of p+.
UK contact 2	1. Measurement of transmit fields produced by 2-D transducer arrays. 2. Diagnostic 3. Absolute pressure values not important. Need linear pressure-voltage relationship over 50 + dB dynamic range. 4. No correction factor. 5. PA HP series probes with submersible pre-amplifier and DC coupler. No knowledge of amp response. 6. No. 7. Possibly.
UK contact 3	1. Pressure/intensity measurements on diagnostic and physiotherapy systems, beam plotting and use in materials characterisation. 2. Diagnostic and therapeutic. 3. ± 5% for pressure, ± 10% for PPSI. 4. No. Only calibration points supplied by NPL. 5. 0.5 mm 50 μm bilaminar, GEC Marconi amplifier type Y-34-9724, PA needle hydrophones and submersible pre-amp/couples. 6. No. 7. Yes.
UK conctact 4	1. Provides acoustic output measurement service for scanners in N. England hospitals (p-, I_{SPTA}, MI). 2. Mainly diagnostic. 3. As good as reasonably achievable. 4. No. 5. In-house system: GEC Marconi pre-amp type Y-33-9724, RS components 50 Ω 0.5 W, 0 to 100 dB attenuator, mini circuits power amp type ZHL-32A. 6. No. 7. Yes.

UK contact 5	1. Use of membrane and needle hydrophones to get waveforms, spectral content and spatial distribution of sound field for bubble sizing and characterisation of signals for pulse propagation through cancellous bone samples and contrast agents. 2. Diagnostic and therapeutic. Lithotripsy in the near future. 3. 10% for ocean applications in pressure. Ideally 2%. 4. Yes. 5. Use NPL calibrated system or system cross-checked against NPL calibrated one. Must assume that phase is linear over frequencies of interest. 6. No. 7. Yes, if true acoustic pressure can be obtained and for an estimate of phase.
UK contact 6	1. Medical diagnostic and therapeutic field measurement: safety and calibration. Experimental studies into non-linear propagation effects. In situ exposure measurements. 2. Diagnostic, physiotherapy, laboratory systems of similar configuration. 3. As accurate as possible. Ability to retain accuracy at higher frequencies is desirable. 4. Needle hydrophones are corrected over their used frequency range. No correction applied to membrane hydrophones: use of amplifier with compensating frequency response. 5. • NPL beam calibrator 1mm spacing, 0.5 mm elements, 0.5 mm 2x25 μm bilaminar with NPL amplifier (calibrated together) (now old). • 9 μm coplanar with 100 MHz buffer amp: flat response up to ≈ 50 MHz (new). • 200 μm PA needle and amp. No amp or phase data. 6. No. 7. Yes.
UK contact 7	1. Provide assessment service for NHS ultrasound equipment in the region. Research into medical ultrasound system and transducer design. 2. Diagnostic (pulsed and continuous wave Doppler) and therapeutic (physiotherapy). 3. Not established 4. No 5. PA needle hydrophone, pre-amp and booster amp. Limited information of magnitude response. 6. No. 7. Yes.

UK contact 8	1. Determine patient exposure, compliance with international standards and provide accurate experimental data to inform models of ultrasonic interactions (e.g. with contrast microbubbles) 2. Diagnostic, therapeutic and surgical ultrasonic fields. 3. Better than 10% is desirable. 4. No. Use best measured estimate (membrane plus matched amp or 2 different types of hydrophone to compare answers) and include estimate of uncertainty. 5. • 2 Marconi 0.5 mm bilaminar membranes, one NPL calibrated (to 20 MHz) with matched amp, the other calibrated similarly with unmatched amp. These are also used with a Rohde & Schwartz RF power meter (manufacturer's calibration only). • 2 Dapco 0.3 mm PZT needle hydrophones (uncalibrated) • 6 PA PVDF needles (one 0.2 needle is NPL calibrated up to 40 MHz) with common pre-amp and wideband amp (uncalibrated). No knowledge of phase characteristics. 6. No. 7. Yes.
UK contact 9	1. Research in lithotripsy cavitation. 2. Diagnostic and lithotripsy. 3. Accurate values for p- required (± 0.5 MPa) 4. Yes. 5. No amplifiers used. Waveform is processed after capture. 6. No. 7. Yes.

European Union contacts

EU contact 1	1. Use of membrane hydrophones as standard devices and for reference measurements. 2. Interest in the complete range of medical ultrasonic fields. 3. Depends on application. 4. In most cases no. Use of complete hydrophone model. 5. In-house amps with know gain. 6. Use of hydrophone model described in: C. Koch and W. Molkenstuck, Trans. UFFC 46 (1999), 1303. 7. See 6.
EU contact 2	1. Perform field measurements for manufacturers to comply with national and international regulations. Use hydrophones in the development for international standardisation. 2. Diagnostic: 1-40 MHz; therapeutic (mainly physiotherapy): 0.8-3.5 MHz; other: bone densitometry, dedicated flow measurements… 3. 12 % for pressures; 25 % for intensities. 4. Usually not (hydrophone bandwidth > 60 MHz). 5. • PVDF, needle type, 0.13 mm diameter, 12cm cable to pre-amp; bandwidth 100 MHz; sensitivity (free-field end-of-cable): 164 nV/Pa at 3 MHz. • PVDF, membrane, 0.4 mm diameter, Sonic pre-amp, bandwidth: 50 MHz; sensitivity (free-field end-of-cable): 36.6 nV/Pa at 5 MHz. • PVDF, needle type, 0.6 mm diameter, 3 cm cable to FET pre-amp used for continuous wave; bandwidth: 50 MHz; sensitivity (free-field end-of-cable): 138 nV/Pa at 1.1 MHz. • NP10, needle type, ceramic active element 0.6 mm diameter, 80 cm cable to Tektronix FET probe P6201 pre-amp used for continuous wave; bandwidth: 25 MHz; sensitivity (free-field end-of-cable): 0.56 nV/Pa at 3.5 MHz. 6. No. 7. Possibly. Depends on information that becomes available (amplitude/phase characteristics).

USA contacts

USA contact 1	1. Use of hydrophones to characterise output of transducers 2. Diagnostic 3. ≈ 10% 4. No. 5. Buffer amplifier (0 dB) with 20 dB gain; phase not measured 6. No. 7. Probably not.
USA contact 2	1. Field measurements for continuous wave and pulsed ultrasonic fields from focused transducers in 0.5-7 MHz range 2. Uses single-element projectors driven with power amplifier, in-house lithotripter and PVDF hydrophones. Does not answer the question. 3. Ideally within 10%. Currently ±20%. 4. No. 5. PA hydrophone into 50 Ω terminated input on a LeCroy digital oscilloscope. Uses Matec 625 amp (flat gain and well-characterised phase in band of interest). 6. No. 7. Yes.
USA contact 3	1. Measurement of fields for regulatory compliance and implementation of the ODS. 2. Diagnostic. 3. As good as possible. 4. Generally no. 5. Approx. 15 Marconi hydrophones with switchable (blue) pre-amps. 6. No. 7. Perhaps.
USA contact 4	1. Reliable and "accurate" measurement of acoustic pressure fields in the kHz up to 50 MHz. 2. Diagnostic and therapeutic. 3. 5-20% for p+ and p-, over field intensities in the 50 kPa – 5 MPa range. 4. No. Use extended calibration points (beyond 1 – 20 MHz) provided by NPL. 5. Broadband (DC - 200 MHz) 50 Ω impedance amplifier, in-line. No knowledge of magnitude and phase characterisitics. 6. No. 7. Yes.
USA contact 5	1. Use hydrophone measurements to characterise and control sound fields for diagnostic ultrasound equipment. Keen interest in behaviour and stability of hydrophones. 2. Diagnostic ultrasound instruments. 3. Maximum uncertainty for pressure measurement: 14%. 4. Correction factor not required at present. 5. Marconi type 699/1/00001/100 hydrophones with matched amplifiers. 0.5 mm elements, bilaminar, PVDF 50 μm total thickness 6. No. 7. Yes.